14

The Lithosphere and Surface of Io

Alfred S. McEwen
University of Arizona

Laszlo P. Keszthelyi
U. S. Geological Survey

Rosaly Lopes
Jet Propulsion Laboratory

Paul M. Schenk
Lunar and Planetary Institute

John R. Spencer
Lowell Observatory

14.1 INTRODUCTION

Io, the innermost of the four large satellites discovered by *Galileo* Galilei in 1610, has a mean radius (1821.6 km) and bulk density (3.53 g cm^{-3}) comparable to the Moon (Anderson *et al.* 2001). However, long before the *Voyager* spacecraft encounters in 1979, Earth-based observations revealed that Io is very different from the Moon: it has an unusual spectral reflectance, anomalous thermal properties, and is surrounded by immense clouds of ions and neutral atoms (Nash *et al.* 1986).

Following closely on the discovery of a thermal "outburst" (Witteborn *et al.* 1979) and the theoretical prediction of intense tidal heating (Peale *et al.* 1979), *Voyager* spacecraft observations revealed a world peppered by active volcanoes (Smith *et al.* 1979). Figures 14.1, 14.2 and 14.3 (Plates 7, 8, 9) show a global image and examples of geological features on Io. A map of Io is shown in Appendix 1 and Plate 16. Many *Voyager*-era investigators, with the most notable exception of Carr (1986), thought that Io's active volcanism was dominated by sulfurous eruptions rather than the silicate volcanism that was common in the inner solar system. *Voyager* lacked the ability to detect the high temperatures (greater than ~800 K) that could distinguish molten or recently molten silicates from molten sulfur or sulfur compounds, but subsequent telescopic and *Galileo* observations have shown that the volcanism on Io is dominated by high-temperature events, very likely eruptions of silicate lava (see reviews by Spencer and Schneider 1996, McEwen *et al.* 2000b, Davies 2001). Some temperature measurements have been even higher than the hottest terrestrial basaltic eruptions and suggest especially Mg-rich compositions (McEwen *et al.* 1998b, Lopes *et al.* 2001a, Davies *et al.* 2001).

Gravity measurements from tracking of the *Galileo* spacecraft indicate that Io has a large iron or iron/iron sulfide core, comprising ~20% of the satellite's mass (Anderson *et al.* 2001, Chapter 13), confirming the prediction of Consolmagno (1981) and the hydrostatic shape measurements of Gaskell *et al.* (1988). Io, however, lacks a strong intrinsic magnetic field, suggesting little core convection (Chapter 21). Io's bulk composition may be close to that of the L and LL chondrites (Kuskov and Kronrod 2000). Sulfur-rich materials, especially SO_2, cover most of the surface. The atmospheric pressure is $\sim 10^{-9}$ bar, but varies spatially and temporally, perhaps influenced by volcanic activity (Chapter 19). Physical and orbital data are summarized in Appendix 2.

The importance of tidal heating in powering Io's enhanced heat flow and active volcanism is widely accepted (Chapter 13). All plausible non-tidal heat sources are about two orders of magnitude less energetic than the power output of Io. The basic tidal-heating mechanism involves deformation of Io into a triaxial ellipsoid by Jupiter's gravitational field (Greenberg 1982). Because Io's orbit is eccentric, forced by orbital resonances among Io, Europa, and Ganymede (Laplace 1805), the satellite undergoes a periodic deformation. Segatz *et al.* (1985) have shown that Io's orbital eccentricity, combined with reasonable parameters for its mantle rheology, can produce energy-dissipation rates as high as 3×10^{15} W, well above Io's current output. However, the transfer of orbital energy from Jupiter to Io is a consequence of the bulge raised on Jupiter by Io, and the rate of such transfer depends inversely on Jupiter's dissipation factor (Q_J). This value is poorly known, but giving Q_J the lowest possible value averaged over 4.5×10^9 years results in an upper limit to Io's average energy dissipation rate of $\sim 4 \times 10^{13}$ W (Peale 1999). Io's power output over the past

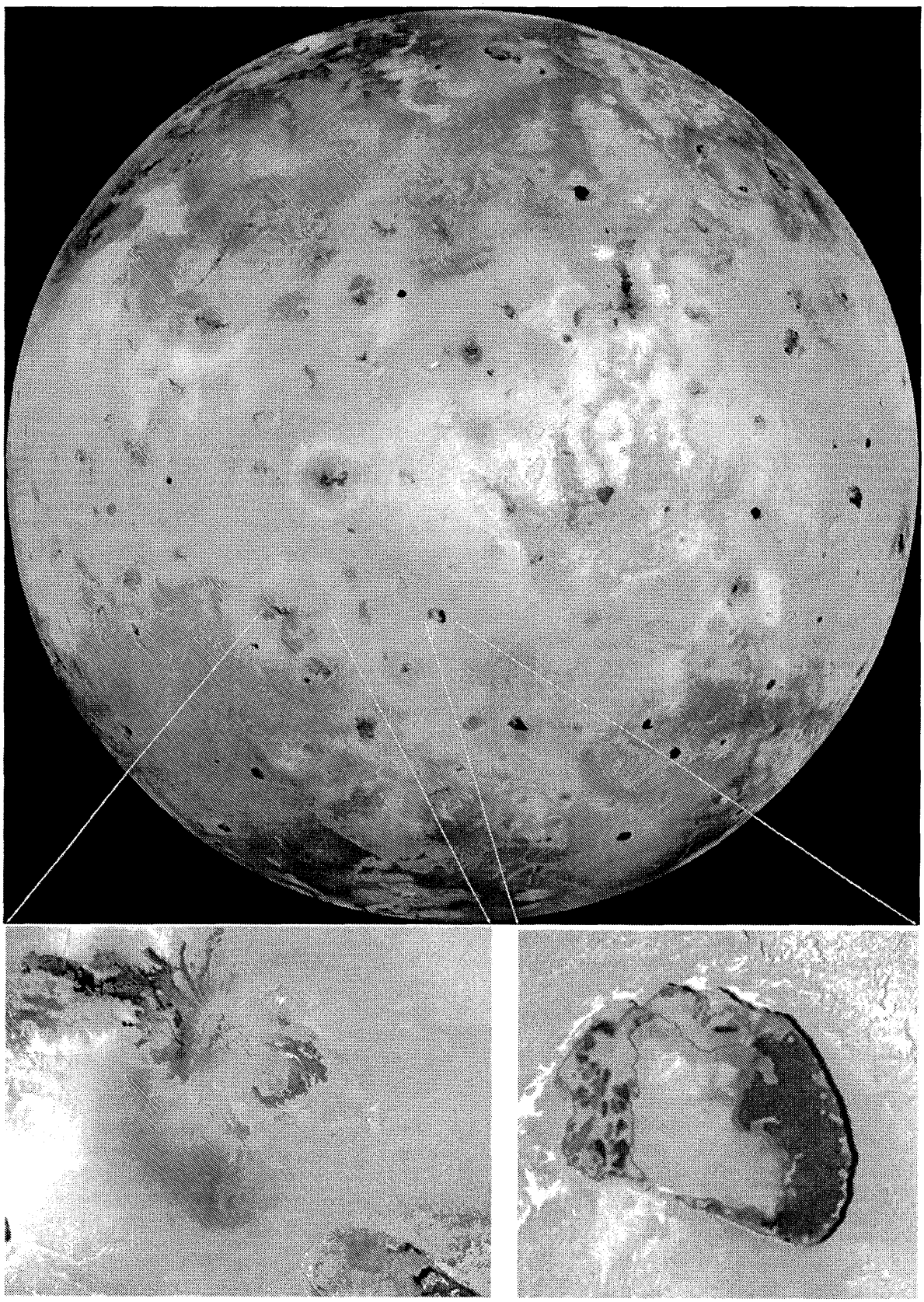

Figure 14.1. Full-disk color mosaic of Io's anti-Jovian hemisphere acquired by *Galileo* in orbit C21, with insets showing high-resolution images of Tupan Patera from orbit C31 (lower right) and Culaan Patera from orbit I25 (lower left). All images are near true-color, but enhance the red colors because the 756-nm filter data was used in place of the red filter. Global image is 1.4 km/pixel, Culann was imaged at 200 m/pixel, and Tupan at 135 m/pixel. North is to the top in all images. At the time of going to press a colour version of this figure was available for download from http://www.cambridge.org/9780521035453.

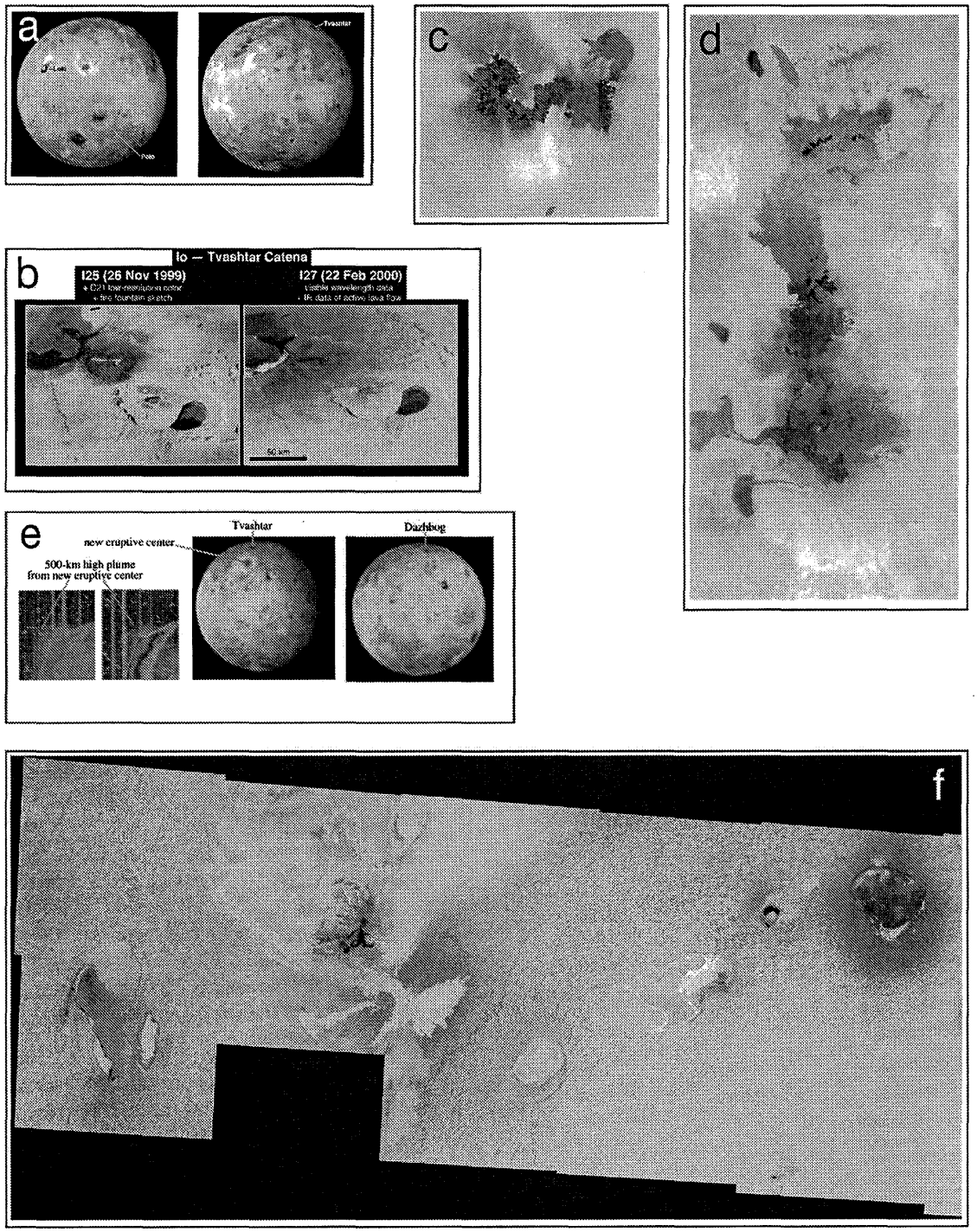

Figure 14.2. Collage of color images of Io. (a) Near-true color *Galileo* SSI images of Io from orbit G29 at a resolution of 10 km/pixel. Note the prominent red rings from the Pele and Tvashtar plumes. (b) Comparison of Tvashtar Catena as seen by *Galileo* SSI in orbits I25 and I27. I25 image has red lava drawn in as inferred from the position of bleeding pixels and colorized using C21 data. I27 image is true color except over the glowing lava which was made visible by overlaying data from SSI's three infrared filters on to the visible image. (c) *Galileo* SSI view of Prometheus Patera and surroundings from orbit I27. Mosaic is at 170 m/pixel and true-color with north to the top. (d) *Galileo* SSI near-true color view of the Amirani flow field from orbit I27. Center of image contains color data at 170 m/pixel, upper and lower parts of the flow field were imaged at 170 m/pixel only in the green filter, and the entire I27 data set was merged with the 1.4 km/pixel C21 global color data for context. (e) *Galileo* SSI views of tall high latitude plumes on Io from orbit I31. Pair of false-color eclipse images on the left are at 18 km/pixel and used the violet filter. Near-true color images on the right are at 19 km/pixel and use the violet, green, and 756-nm filters. (f) *Galileo* SSI view of the Chaac–Camaxtli region at 180–185 m/pixel from orbit I27. I27 data was collected in the clear filter then merged with the 1.4 km/pixel C21 global color data. At the time of going to press a colour version of this figure was available for download from http://www.cambridge.org/9780521035453.

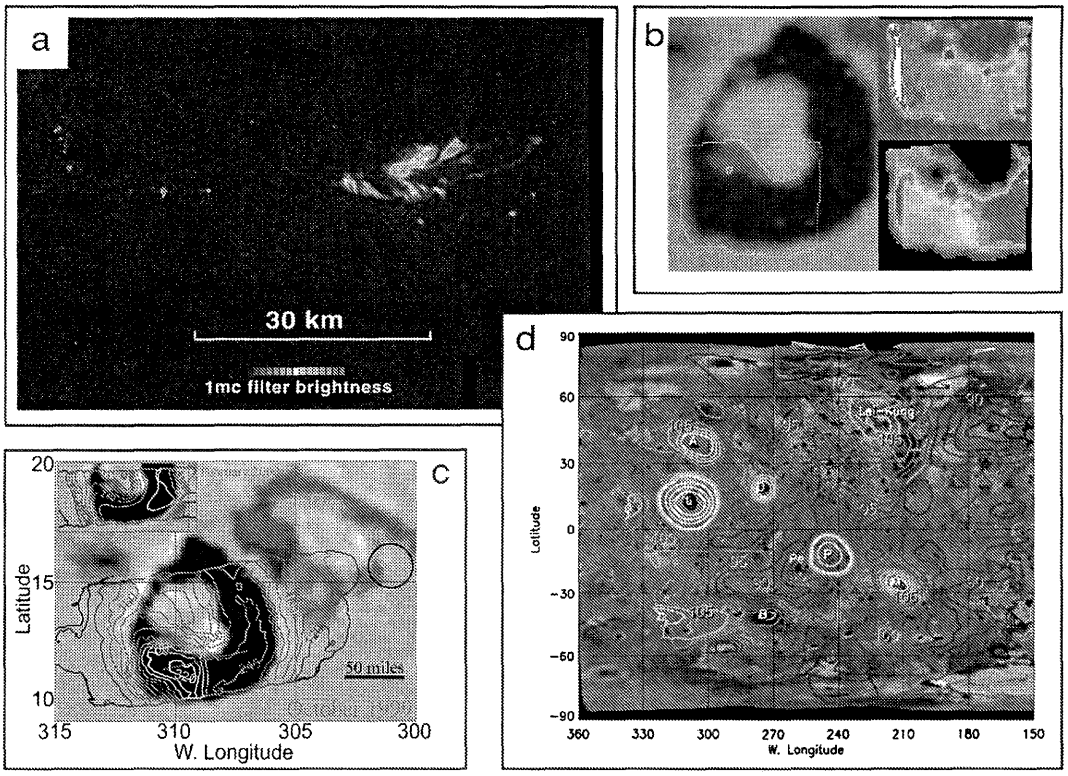

Figure 14.3. Collage of color images of Io. (a) *Galileo* SSI nighttime 1 μm brightness image of Pele Patera from orbit I32. Image is at 60 m/pixel. (b) *Galileo* PPR nighttime temperature map of Loki Patera and surroundings from orbit I24. (c) *Galileo* NIMS nighttime brightness temperature maps of Loki Patera from orbit I32. Upper map is at 2.5 microns and lower map is at 4.4 microns. (d) PPR nighttime temperature map of a hemisphere of Io using data from orbits I25 and I27. A = Amaterasu, D = Daedalus, L = Loki, P = Pillan, Pe = Pele, M = Marduk, B = Babbar. At the time of going to press a colour version of this figure was available for download from http://www.cambridge.org/9780521035453.

20 years ($\sim 10^{14}$ W, as described below) exceeds this upper limit.

The mechanism of heat dissipation is intimately tied to Io's internal structure. The initial model suggested by Peale *et al.* (1979) – i.e., "runaway" melting of the interior leading to tidal energy dissipation within a thin (8–18 km) elastic lithosphere – seems inconsistent with the presence of mountains more than 10 km high (Smith *et al.* 1979). Furthermore, it is now clear that most or nearly all of Io's tidally generated heat is transferred to the surface via silicate magma, not conduction through the lithosphere.

Previous review papers about Io's surface and lithosphere were published before the *Galileo* mission (Nash *et al.* 1986, McEwen *et al.* 1989, Spencer and Schneider 1996), or written prior to the acquisition of high-resolution *Galileo* observations (McEwen *et al.* 2000b) or the latest flybys (Davies 2001). In this short review we will focus on new results and synthesis from the close *Galileo* flybys in 1999–2002 (Table 1) and other recent results.

The success of *Galileo*'s close encounters with Io was limited by the damaging effects of Jupiter's intense radiation environment on the spacecraft electronics (Erickson *et al.* 2000). There were six close flybys late in the mission (Table 1); orbits are denoted as "I24" for an Io flyby on *Galileo*'s 24th orbit, etc. Many of the observations planned for orbits I25 and I33 were lost when problems caused the spacecraft to enter "safe mode." In addition, parts of the Ultraviolet Spectrometer (UVS) and the Near Infrared Mapping Spectrometer (NIMS) were damaged prior to I24. Close-up NIMS observations of Io were possible at only a dozen wavelengths (Lopes-Gautier *et al.* 2000). The Solid State Imager (SSI) was first degraded only in summation mode (used extensively in I24; see Keszthelyi *et al.* 2001) and later experienced other problems, which eliminated most images from I31. Although the Photopolarimeter-Radiometer (PPR) experienced difficulties early in the mission, it was trouble-free during the close Io flybys (Spencer *et al.* 2000b, Rathbun *et al.* 2002). The valiant efforts of the *Galileo* engineers led to workarounds for many problems, and two flybys (I27 and I32) were highly successful.

14.2 COMPOSITION OF IO'S SURFACE, CRUST, AND MANTLE

14.2.1 Surface Composition

The uppermost layer of Io's surface is largely coated by volatile compounds, most likely the result of volcanic gas release. Spectroscopy of the surface is dominated by these "painted on" coatings and the measurements are more diagnostic of the volatile components than of the bulk composition of the crust. Nevertheless, the current volatile inventory is an important constraint on models for the evolu-

Table 14.1. Close flybys of Io by the *Galileo* spacecraft.

Flyby	Date	Observation Difficulties	Major Results
J0	Dec 1995	No remote sensing of Io.	Fields and particles results (see Chapters 21–27).
I24	Oct 1999	Most SSI images scrambled, but many were reconstructed.	First close look at Io's surface and hot spots.
I25	Nov 1999	Close-approach sequence lost due to spacecraft safing, but good medium-resolution data obtained.	Tvashtar Catena curtain of lava; regional temperature maps.
I27	Feb 2000	None – fully successful.	Many new results on lava flows, mountains, paterae, and heat flow.
I31	Aug 2001	Most SSI images lost, good data from PPR, NIMS, and fields and particles instruments.	Evidence for four major new plume eruptions in north polar region.
I32	Oct 2001	None – fully successful.	Many new results, including absence of intrinsic magnetic field.
I33	Jan 2002	All Io observations (except PPR nightside) lost due to spacecraft safing.	PPR temperature maps.

tion of Io's interior and volcanic processes. In spite of much improved data collected since the *Voyager* era, SO_2 is still the only compound that has been definitively identified on Io's surface, and elemental sulfur is still suspected to be a major component (Nash *et al.* 1986). Extensive coverage of the surface by SO_2 and its numerous and strong absorption bands in the infrared make detection straightforward compared with other possible compounds. Evidence of other volatile compounds is provided by the following:

(i) The identification of neutral and ionized SO_2, SO, S, O, Na, Cl, and K in the Io torus and neutral clouds (Chapter 23);

(ii) The variety of surface colors and spectral shapes at ultraviolet–visible wavelengths that match sulfur allotropes (e.g., Soderblom *et al.* 1980, Moses and Nash 1991);

(iii) The detection of S_2 in the Pele plume (Spencer *et al.* 2000b);

(iv) The detection of absorptions in the infrared that cannot be attributed to SO_2 (e.g., Salama *et al.* 1990, Carlson *et al.* 1997, Schmitt *et al.* 2002); and

(v) The detection of hydrogen (Frank and Patterson 1999) and hydrogen sulfide (Russell and Kivelson 2001) in Io's exosphere.

Sulfur Dioxide

The global distribution of SO_2 on Io's surface results from volcanic venting of gaseous SO_2 into the plumes and atmosphere. SO_2 is subsequently deposited on to the colder surfaces as frost. Some SO_2 frost sublimates when exposed to sunlight, supplying additional SO_2 to the atmosphere, but nighttime temperatures probably cause SO_2 to condense back on to the surface (e.g., Ingersoll 1989, Chapter 19). Measurements by *Voyager*'s Infrared Interferometric Spectrometer (IRIS) (Pearl *et al.* 1979) provided the first direct detection of gaseous SO_2 from one of Io's volcanic plumes (Loki). Detection of sulfur dioxide frost on Io's surface was provided by ground-based 4-micron spectroscopy (Smythe *et al.* 1979, Fanale *et al.* 1979). Before *Galileo*'s arrival at Jupiter, the distribution of SO_2 on Io's surface was mapped using ultraviolet and visible reflectance measurements (Nash *et al.* 1980, Nelson *et al.* 1980, McEwen *et al.* 1988, Sartoretti *et al.* 1994) and using infrared spectroscopy (Howell *et al.* 1984). These studies resulted in some conflicting views on the SO_2 distribution and abundance.

Initial NIMS results for Io's anti-jovian hemisphere showed that SO_2 frost is present almost everywhere on the surface, but larger grain sizes are found near the equatorial regions (Carlson *et al.* 1997, Appendix 1). The only areas lacking SO_2 are those in the vicinity of hot spots, where surface temperatures are sufficient to vaporize or prevent condensation of SO_2. Douté *et al.* (2001a) showed that SO_2 is most prevalent in several large areas at middle latitudes. Extended areas depleted in SO_2 are also found, especially in the longitude range 270–320 degrees. The regions with abundant SO_2 (surface coverage >60%) show a longitudinal correlation with plumes located close to the equator.

Douté *et al.* (2001a) proposed that most of the SO_2 gas from the plumes (located mainly in the equatorial regions) flows towards colder surfaces at higher latitudes. A small fraction of the SO_2 settles on to cold equatorial regions. The spectral signature of SO_2 in the equatorial regions is significantly stronger, consistent with larger grain sizes. Sunlight causes condensed SO_2 frost at low latitudes to undergo slow metamorphism and sublimation, creating deposits with large effective grain sizes. SO_2 deposits at medium and high latitudes may be optically thin (Simonelli *et al.* 1997, Geissler *et al.* 2001). The weaker SO_2 spectral signature at medium and high latitudes may be due to rapid radiolytic destruction of condensed SO_2, leaving residual SO_2 deposits over darker radiolytic products (Wong and Johnson 1996, Carlson *et al.* 2001, Chapter 20).

Galileo's close flybys of Io provided the opportunity to study the distribution and physical properties of SO_2 at small spatial scales and close to hot spots and plumes. A bright white area inside Baldur Patera (Figure 14.2f) corresponds to a 90% to 100% concentration of SO_2 (Lopes *et al.* 2001a). Higher concentrations of SO_2 do not necessarily correspond to bright white surfaces seen at low phase angles. High-resolution observations of the Prometheus hot spot and plume site by NIMS showed an SO_2 plume deposition ring (Lopes-Gautier *et al.* 2000, Douté*et al.* 2002) that extends beyond the bright white ring seen in visible low

phase images (but matching that seen at moderate phase angles; Geissler *et al.* 2001).

Elemental Sulfur

Sulfur as a free element is thought to be common on Io's surface. Io's full-disk reflectance spectrum cannot be explained by SO_2 alone, and requires the addition of a material like elemental sulfur that absorbs in UV and blue light but is highly reflective and featureless in the near-IR (Fanale *et al.* 1982). Although some researchers have argued against the presence of elemental sulfur on Io (Young 1984, Hapke 1989), experimental work by Moses and Nash (1991) supported the presence of metastable sulfur allotropes on the surface. In particular, they argued that polymeric sulfur is probably very stable at Io surface conditions and, once formed, can persist indefinitely. More recently, Kargel *et al.* (1999) argued that impure sulfur of volcanic origin has spectral properties consistent with much of Io's surface and is more likely to be present than pure elemental sulfur.

The best evidence for elemental sulfur on Io comes from the direct detection of gaseous S_2 in the Pele plume by the Hubble Space Telescope (HST) (Spencer *et al.* 2000a). The Pele plume deposits are bright red; Spencer *et al.* suggested that red S_3 and S_4 molecules are produced by polymeralization of S_2. Red deposits (Plates 7, 8, 9) are commonly associated with active volcanoes and appear to fade with time if volcanic activity wanes (Spencer *et al.* 1997a, McEwen *et al.* 1998a, Geissler *et al.* 1999). The spectral properties of these deposits are consistent with short metastable sulfur chains (e.g., S_3, S_4) mixed with elemental sulfur or other sulfurous materials. With time, S_3/S_4 further polymerizes into the more stable cyclooctal S_8, turning the color of the deposits from red to pale yellow. By analogy with Pele and an association with vent structures, other red deposits are interpreted to be indicators of S_2 venting. Some red deposits (e.g., near Culann, Figure 14.1 and Plate 7) show enhanced concentrations of SO_2 (Lopes-Gautier *et al.* 2000). Spencer *et al.* (2000a) observed that SO_2 was more abundant than S_2 in the Pele plume, and one possibility is that SO_2 condenses on S_2 solid nuclei and they are deposited together in an intimate mixture.

Two other spectral units on Io may be composed of sulfur in some form:

(i) Greenish materials are seen on Io; they have a negative spectral slope from 0.7 to 1.5 μm (Geissler *et al.* 1999, Lopes *et al.* 2001a) that is not characteristic of pure sulfur or SO_2 compounds. The green color is restricted to dark patches (probably the crusted surfaces of recent lava flows and lava lakes), and red materials deposited on recent lavas have later turned green (Keszthelyi *et al.* 2001), so the green color may be due to contamination or alteration of the red material by the warm silicate lavas.

(ii) There is a broad absorption feature of unknown origin in the 1–1.3 μm region of Io's spectrum (Pollack *et al.* 1978, Carlson *et al.* 1997). NIMS data show an anti-correlation between this absorption and recent lavas that are either dark or greenish at visible wavelengths (Lopes *et al.* 2001a). The spectral feature does correspond to dark polar regions (Carlson *et al.* 2001). Suggestions for its origin include sulfur–iron compounds such as pyrite (Kargel *et al.* 1999); short-chain sulfur allotropes or sulfanes, produced in the radiolysis of SO_2 (Carlson *et al.* 2001); and sulfur contaminated by trace elements (Douté *et al.* 2001b).

Other Compounds

A few absorption features have been attributed to compounds other than SO_2, including H_2S (Nash and Howell 1989), SO_3 (Nelson and Smythe 1986, Khanna *et al.* 1995), and H_2O and H_2S frozen in SO_2 (Salama *et al.* 1990). Salama *et al.* reported weak absorption features at 3.85 μm and 3.91μm (H_2S) and 2.97 μm and 3.15 μm (H_2O). The 3.15 μm feature was confirmed in NIMS spectra by Carlson *et al.* (1997), who interpreted this feature as possibly caused by the O–H stretch transition, implying hydrated minerals, hydroxides, or possibly water. When seen at higher spatial resolution the band at 2.97 μm is well modeled by pure SO_2 ice (Coustenis *et al.* 2002). Shirley *et al.* (2001) identified a broad absorption from 3.0–3.4 μm and suggested that it might be related to hydrogen-bearing species, including H_2O. Chlorine compounds Cl_2SO_2 or $ClSO_2$, mixed with SO_2, have been suggested by Schmitt and Rodriguez (2002) as explanations for an absorption band at 3.92 μm (likely the same band detected by Salama *et al.* 1990, at 3.91 μm).

Hydrogen-bearing species, particularly H_2O, are major constituents of terrestrial volcanic gasses. However, Io is thought to have lost nearly all of its hydrogen because of its highly evolved state (Zolotov and Fegley 1999). The detection of hydrogen pickup ions by *Galileo*'s plasma analyzer (Frank and Patterson 1999) led to the interpretation that Io may provide a flux of hydrogen from the surface to the atmosphere, as hydrogen escapes rapidly to space. It is also possible that the source of the hydrogen is the jovian magnetosphere, not Io. Thermochemical equilibrium calculations by Zolotov and Fegley showed that H_2O is likely to be the dominant hydrogen-bearing gas, followed by H_2S, HS, H_2, NaOH, KOH, and HCl. Dissociation of volcanic H_2O by photolysis and radiolysis could produce the atomic hydrogen observed (Johnson 1990, Johnson and Quickenden 1997, Chapter 20).

14.2.2 Composition of Io's Crust and Mantle

Io's bulk density and moment of inertia and the chemistry of the solar system indicate that the satellite's mantle and lithosphere are composed of silicates (Chapter 13). Many previous workers have assumed that Io has a crust (i.e., a region of lower-density petrology differentiated from a higher-density mantle), which may or may not correspond to the lithosphere (i.e., a rigid outer shell, irrespective of its composition). Provided that Io's crust is composed primarily of a thick stack of lavas (e.g., Carr *et al.* 1998), it may be possible to determine the dominant composition of Io's upper crust from the compositions of the lavas exposed on the surface.

Bright, sulfurous materials cover most of Io, except on relatively small areas where the dark and recent silicate lavas are exposed. Since NIMS was damaged prior to the I24 encounter, observations resolving the dark lavas at high spectral resolution have not been possible. Only SSI (with six color band passes) has fully resolved the dark lavas, detecting an absorption feature at ~0.9 μm (Geissler *et al.* 1999).

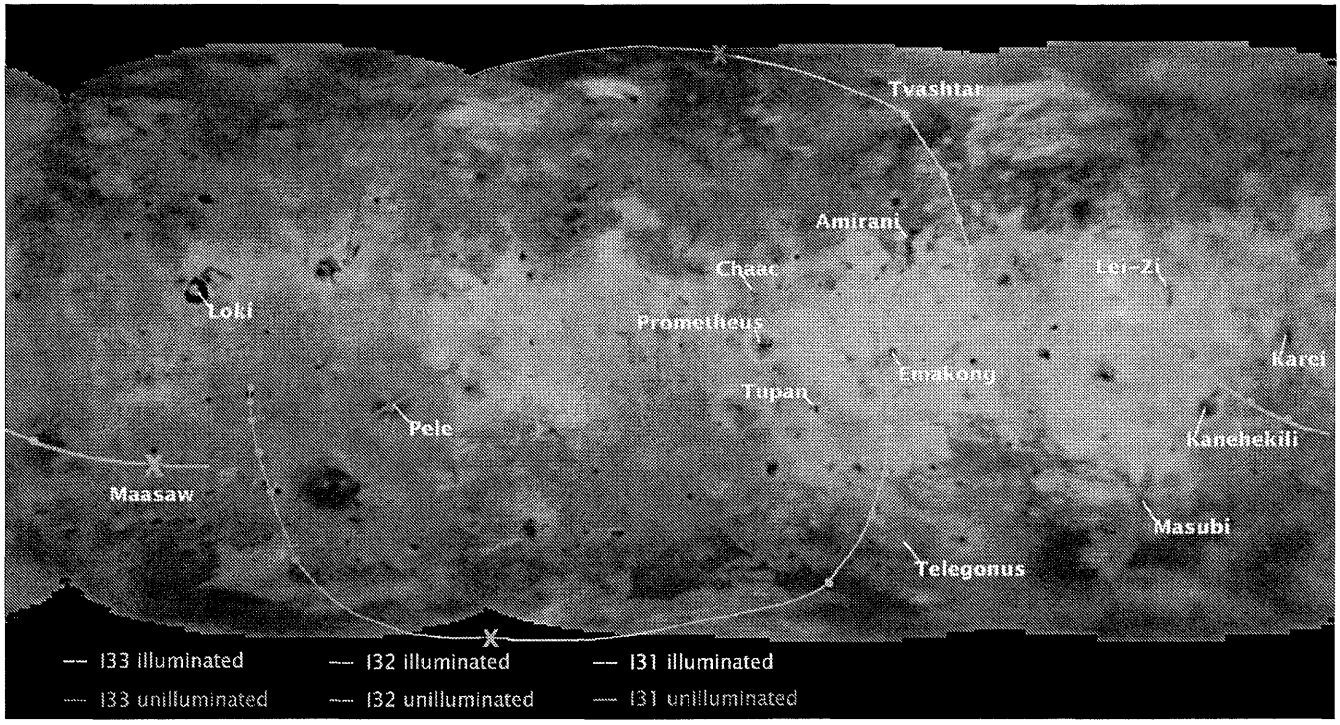

Figure 14.4. Global map showing locations of features named in the text. Lines show path of *Galileo* over Io during the last 3 close flybys (orbits I31, I32, and I33); "X" mark locations of closest approach.

This color signature is consistent with relatively iron-poor orthopyroxenes – i.e., Fe/Mg-rich silicate minerals common in terrestrial mafic and ultramafic lavas. Mg-rich compositions are consistent with the very high eruption temperatures measured on Io and with a prediction of magnesium-rich pyroxenes in Io's mantle (Keszthelyi *et al.* 1999).

Nearly all of the low-albedo lavas observed through SSI near-IR filters have the 0.9 micron absorption, suggesting that lavas with Mg-rich orthopyroxene are common, and that the entire crust may have a mafic or ultramafic composition. The high temperatures detected at a number of Ionian eruptions are consistent with Mg-rich lava compositions. In addition, the very low slopes of lava flows (Schenk *et al.* 1997, 2003) and lack of steep-sided volcanoes are inconsistent with viscous lavas. Siliceous lavas are expected to be highly viscous, whereas mafic lavas are usually very fluid, unless rich in crystals. These observations are difficult to reconcile with the low-density alkalic and siliceous crust expected to result from repeated partial melting in a solid mantle (Keszthelyi and McEwen 1997) and requires that the crust is somehow efficiently recycled back into the mantle (Carr *et al.* 1998).

14.3 ACTIVE VOLCANISM OF IO

Voyager and *Galileo* images have revealed many active plumes, lava flows, and volcano–tectonic depressions called paterae (see Figures 14.1 through 14.5). Infrared observations have revealed many hot spots, all closely corresponding to dark areas that are probably largely free of sulfurous coatings (McEwen *et al.* 1997). Shield volcanoes or stratocones like those on Earth are rare. Nearby mountains appear to be tectonic structures rather than volcanoes, with a few exceptions. Only a few shield-like cones have been directly observed (e.g., Zamama, Figure 14.5), although radially-oriented flow fields suggest the presence of low shields with very shallow slopes (Schenk *et al.* 2003).

14.3.1 Silicate Volcanism

Galileo and telescopic observations of Io have revealed a wide range of eruption rates, eruption styles, thermal characteristics, and lava morphologies (e.g., Spencer *et al.* 1997b, Davies 2001; Keszthelyi *et al.* 2001, Lopes *et al.* 2001a). Most high-temperature hot spots occur on patera floors. There are also a number of large active lava flow fields (flucti) such as Amirani-Maui, Culann, and Prometheus (Figures 14.1, 14.2). The very largest dark flow field, Lei Kung Fluctus (Figure 14.3), must have been emplaced in recent decades because it remains a large low-temperature thermal anomaly (Spencer *et al.* 2000b). Despite the variations in Ionian volcanism, some broad generalizations can be drawn. The majority of Ionian eruptions can be placed into one of three classes: "Promethean" and "Pillanian" after type examples seen by *Galileo* (Keszthelyi *et al.* 2001), and lava lakes.

Promethean Volcanism

These volcanic centers have long-lived, compound flow fields fed by insulated lava tubes or sheets. Examples of Promethean eruptions include the activity at Prometheus, Culann, Zamama, and Amirani (Figures 14.1 and 14.2); all are "persistent" hot spots as defined by Lopes-Gautier *et al.* (1999). Analysis of low-resolution NIMS data for persistent hot spots yielded a mass eruption rate of ~43 km^3/yr and

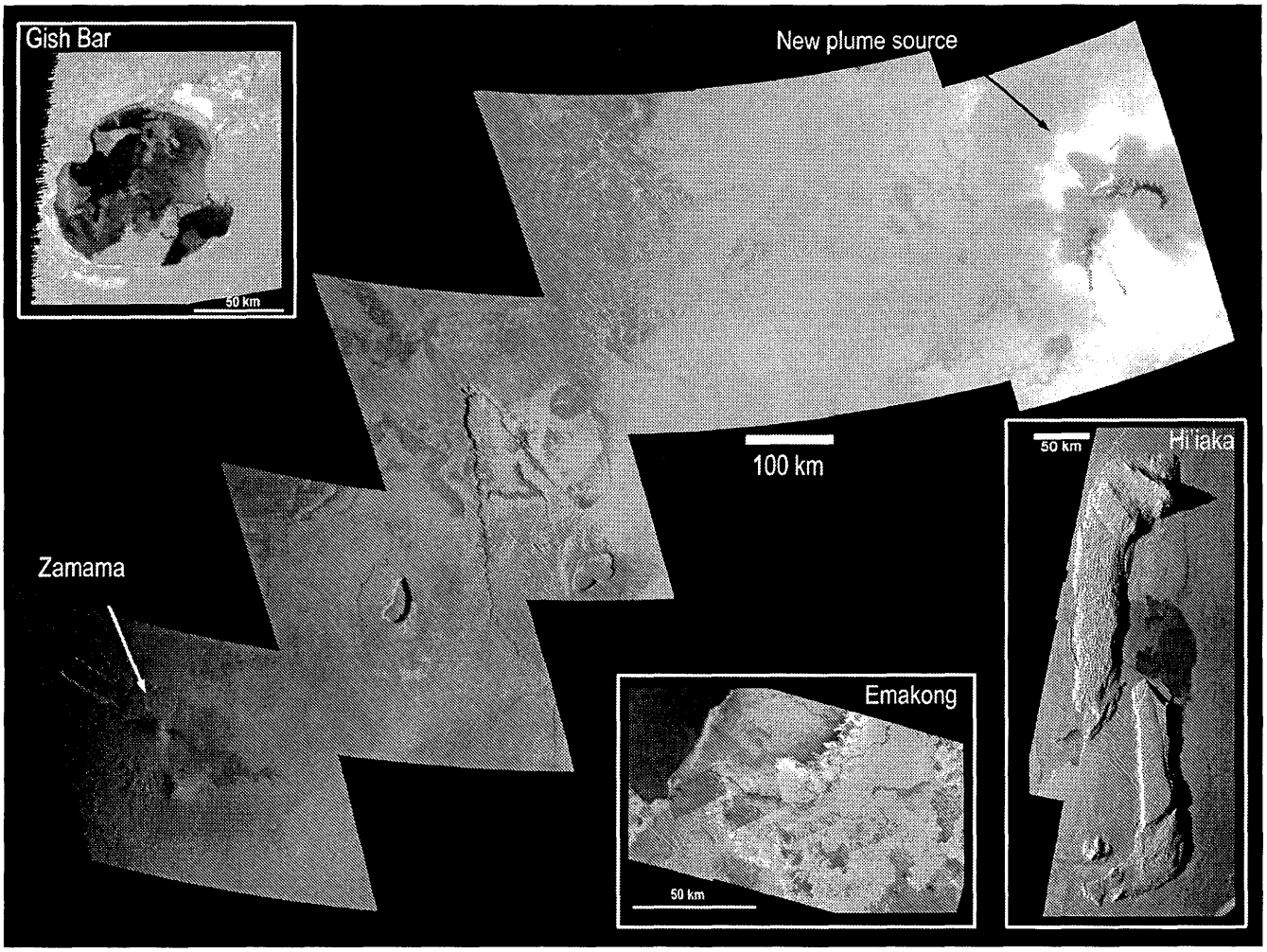

Figure 14.5. Active volcanic centers: Zamama, Gish-Bar Patera, Emakong Patera, Hi'iaka Patera and Mons, and new I31 plume source. The Gish-Bar image and the large mosaic were obtained on orbit I32. The Emakong and Hi'iaka images are from orbit I25. The two large dark regions in Gish-Bar resulted from eruptions sometime from July to October of 1999 (lower right) and between October 1999 and October 2001 (upper left).

a global resurfacing estimate of 0.1 cm/year (Davies *et al.* 2000). Images of the flow fields from different *Galileo* orbits have allowed minimum resurfacing rates to be estimated at Prometheus and Amirani. The active region of the ~100-km-long Prometheus flow field (Figure 14.2c) showed about 0.5 km^2/day of new lava exposed and old lava covered while 5 km^2/day of new lava was seen at the ~300-km-long Amirani flow field (Figure 14.2d, McEwen *et al.* 2000a, Keszthelyi *et al.* 2001). Evidence for insulating lava transport comes not only from the morphology of the lavas, but also from the spatial distribution of thermal emission along the length of the flow fields (Lopes *et al.* 2001a). The lengths of the flows can be hundreds of kilometers and the morphology of the flows is suggestive of pahoehoe (low-viscosity lava textured like rope). Eruptions seem to be able to continue for at least 20 years (McEwen *et al.* 1998a). Lava temperatures obtained to date are consistent with basaltic compositions (Lopes-Gautier *et al.* 2000), but ultramafic compositions cannot be excluded because remote measurements provide only minimum temperatures for the liquid, especially for this style of volcanism.

Pillanian Volcanism

Pillanian eruptions share several key characteristics: a short-lived intense episode with high-temperature, fissure-fed eruptions producing both plumes with extensive pyroclastic deposits and rapidly emplaced lava flows with open channels or sheets. Examples of Pillanian eruptions are Pillan (Davies *et al.* 2001, Williams *et al.* 2001a), Tvashtar (McEwen *et al.* 2000a), Surt (Marchis *et al.* 2002), and the intense new hot spot and plume discovered during orbit I31 (Lopes *et al.* 2001b; see Figure 14.5). In each of these cases, the plume deposits were several hundred kilometers in diameter and composed of white, yellow, red, and/or dark gray materials. (The initial Tvashtar deposits seen in *Galileo*'s orbit I25 were only about 60 km in diameter, and the larger plume and its red deposits were discovered more than a year later.) These types of eruptions often correspond with the "outbursts" seen by ground-based telescopic observers (e.g., Stansberry *et al.* 1997, Howell *et al.* 2001, Marchis *et al.* 2002). However, many outbursts occur from eruptions that do not produce discernable pyroclastic deposits, such as that at Gish-Bar Patera (Figure 14.5). To date, the highest lava

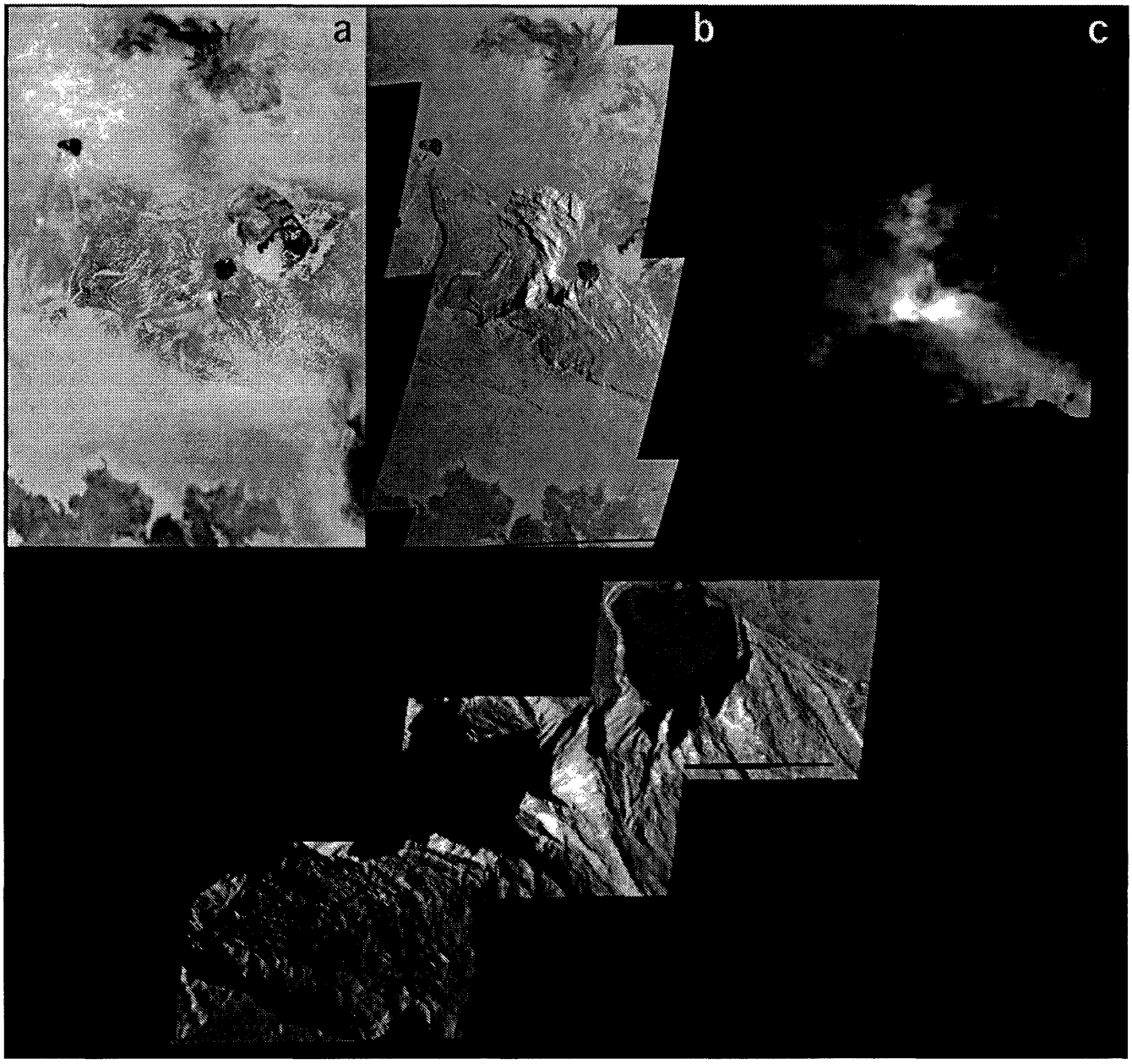

Figure 14.6. Four views of Tohil Mons. Most mountains are not prominent in low phase angle observations; image (a), combining low resolution context imaging from orbit I21 and medium resolution images from I27, reveals bright and dark patterns, some of which correspond to topographic ridges. Low-sun I32 images of Tohil Mons (b) reveal a complex structure consisting of a low, ridged plateau to the east and rugged lineated plateau to the northwest, separated by a complex set of amphitheatres and ridges. (c) is an elevation model derived from stereo analysis by Schenk *et al.* (2001), showing a maximum relief of ~9 km occurs along the central ridge complex. A high resolution (~50 meters/pixel) image swath (d) was obtained along the central section. These images show flow-like morphologies, tentatively interpreted as additional evidence for slope failure on Io.

temperatures have been observed from Pillanian/outburst activity (e.g., Veeder *et al.* 1994, Stansberry *et al.* 1997, McEwen *et al.* 1998b, Davies *et al.* 2001, Marchis *et al.* 2002) with the exception of Pele. These vigorous eruptions expose large amounts of liquid lava, providing a better opportunity to remotely estimate lava temperatures than at Promethean eruptions. It is possible that a Pillanian phase could switch to a Promethean style of eruption or vice versa; Pillan itself has been a persistent hot spot before and after the summer of 1997 event (Lopes-Gautier *et al.* 1999; Davies *et al.* 2001).

Pele, Loki, and Other Potential Lava Lakes

A third class of eruptions fit neither the Pillanian or Promethean categories. These volcanic centers are paterae that contain hot spots and dark lava, and may contain active (convecting) lava lakes. Pele and Loki are the best-studied examples and demonstrate two very different styles of activity that are both consistent with active lava lakes. These two persistent volcanic centers have little else in common other than being the first sites of active volcanism on Io to

be discovered from *Voyager* observations (Morabito *et al.* 1979).

The 186 × 221 km Loki Patera (Figure 14.2b,c) is one of the largest patera on Io while Pele Patera is a bit smaller than average at 19 × 29 km. Loki is the most thermally energetic hot spot on Io with modeled eruption rates $\sim 10^4$ m^3 s^{-1} while Pele has modeled eruption rates of only ~ 300 m^3 s^{-1} (Davies *et al.* 2001). Pele is at the center of a long-lived, ~1400-km-diameter red plume deposit. There was no plume associated with Loki Patera during *Galileo*'s monitoring. There were two active plumes north of Loki Patera in 1979 but these were probably due to active lava flows outside Loki Patera. There are no recent lava flows extending outside of either Loki or Pele Patera (but see Emakong Patera in Figure 14.5 for a possible lava lake that filled up and overflowed the patera). *Galileo* detected very high temperatures within Pele Patera (Lopes *et al.* 2001a, Radebaugh *et al.* 2002). In contrast, temperatures above about 1000 K have not so far been detected at Loki, except perhaps for the poorly located 1990 outburst with a model temperature of 1225 K (Veeder *et al.* 1994, Davies 1996). Despite all these differences, both paterae are thought to contain active lava lakes.

Voyager data analysis led to the suggestion that the Pele hot spot is a silicate lava lake (Howell 1997) and that Loki houses a sulfur lake, maintained liquid by underlying hot silicates (Lunine and Stevenson 1985). The temperatures detected at Loki since 1985 are too high for sulfur, but ground-based and *Galileo* results lend new support to the hypothesis that both these paterae contain silicate lava lakes. Analysis of *Galileo* observations from September 1996 through May 1999 showed that Pele exhibits a nearly constant thermal output, with thermal emission spectra consistent with an active lava lake (Davies *et al.* 2001). During the I24, I27, and I32 *Galileo* flybys, SSI imaged Pele in darkness, showing glowing patterns interpreted as the active fountaining and margins of a lava lake (McEwen *et al.* 2000a, Radebaugh *et al.* 2002). Zolotov and Fegley (2000) modeled the temperature and oxidation state of Pele's magma and exsolved gas based on HST observations of gas chemistry; their results are consistent with Mg-rich lavas.

Loki is the hot spot most easily monitored from Earth. *Voyager* images showed a dark patera floor surrounding a bright "island" or plateau. Observations of Loki during the *Galileo* flybys (Lopes-Gautier *et al.* 2000, Spencer *et al.* 2000b) showed that the dark floor is covered by warm material, while the "island" is cold (Figure 14.3b). The dark material was interpreted as either the cooled crust of a lava lake or cooling flows covering a caldera floor. Ground-based data on Loki's activity obtained over several years showed patterns of infrared brightening and fading with a roughly 540-day period, which Rathbun *et al.* (2002) interpreted as the surface of a periodically overturning lava lake. PPR data obtained during I24 and I27 (Spencer *et al.* 2000b) and NIMS data obtained during I32 (Figure 14.3c) are consistent with this model (Lopes *et al.* 2002). The hottest areas observed by NIMS are located on the southwest corner of the patera, where Rathbun *et al* (2002) suggested the crust first founders and the resurfacing wave starts. Immediately to the east of this area NIMS shows a colder region, probably the oldest crust resulting from the previous resurfacing wave.

Thus the interpreted style of activity of the Pele and Loki lava lakes differ substantially, with the resurfacing at Loki happening quasi-periodically over a huge area and with great heat flow, while at Pele the resurfacing appears to be more continuous and spatially confined, and is associated with a giant plume rich in SO_2 and short-chain sulfur (Spencer *et al.* 2000a). It is not yet known what processes control the different behaviors of these (possible) lava lakes. It is plausible that Pele has a continuous cycling of fresh magma into the lake while Loki is losing heat in a more passive manner. The overturning of lava crust at Loki might be inevitable as the surface cools and becomes denser than the underlying liquid.

There may be many more lava lakes on Io, in various stages of activity, such as Tupan Patera (Figure 14.1), Gish-Bar and Emakong Paterae (Figure 14.5), the patera cut into Tohil Mons (Figure 14.6), and the small dark patera shown in Figure 14.7. Many paterae have floors that are dark and there are persistent hot spots (but without sufficient energy for periodicity to have been detected via ground-based monitoring). SSI images showed no large-scale surface changes following several thermal enhancements observed from Earth, consistent with overturning lava lakes or topographically confined lava flows. However, lava flows are most likely propelled to the surface by expanding volatiles, and should produce abundant pyroclastics in the near-vacuum environment of Io. The lack of plume deposits is consistent with degassed lava in lava lakes. A combination of overturning lava lakes and new lava flows on patera floors is also possible. If a significant fraction of Io's heat flow is due to lava lakes (Loki alone supplies ~15–20%), then the plains covering ~90% of the surface must have a resurfacing rate significantly below the global average, which in turn affects the thermal gradient and structure of the lithosphere.

14.3.2 Plumes

Some of the most dramatic phenomena on Io are the active volcanic plumes. Nine eruption plumes were observed during the *Voyager 1* and *2* encounters (Strom and Schneider 1982). *Galileo* has observed a total of 12 plumes, four of which appear related to *Voyager*-era plumes, so there are a total of 17 volcanic centers with observed plumes. New ring-shaped surface deposits suggest that other plumes have been active as well. Many of the plumes are 50–150 km tall, active for years or decades, deposit bright white material, and are associated with Promethean volcanism. Several of these "Prometheus-type" plumes show signs of lateral migrations over time of up to 100 km, associated with advance of the lava flows (McEwen *et al.* 1998a). Pele's plume is very different from Prometheus-type plumes, as it is very faint at visible wavelengths, up to 460 km high, and deposits bright red material. The existence of many much smaller plumes was hypothesized from *Voyager* observations of small, diffuse, bright streaks radial to Pele (Lee and Thomas 1980), but *Galileo* has not confirmed this prediction.

The dominant volatiles driving explosive volcanism on Earth, H_2O and CO_2, seem to be highly depleted on Io. There is preliminary evidence for small quantities of H, but C has not been detected, even in Jupiter's magnetosphere near Io. In contrast, SO_2 is ubiquitous over the surface and is widely believed to be the dominant atmospheric component (McGrath *et al.* Chapter 19). Hence, volatiles such as SO_2

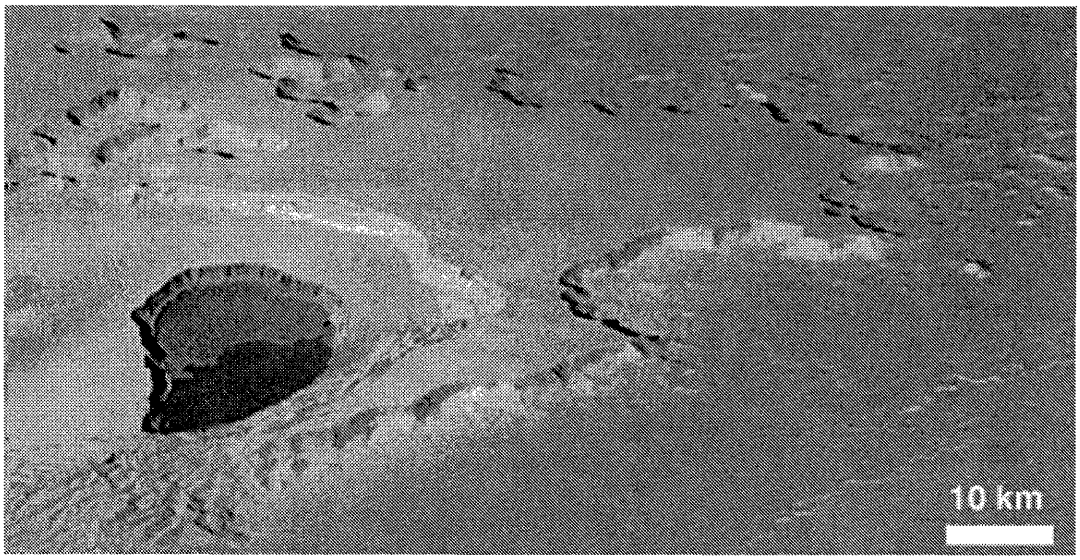

Figure 14.7. Sapping terrain near Tvashtar Catena. Image is from orbit I25 with a resolution of 185 m/pixel and taken through the clear filter.

and sulfur probably drive the explosive volcanism (Kieffer 1982).

Galileo has revealed much about the geologic associations of the plumes. The Prometheus-type plumes generally form over the distal ends of extensive flow fields (McEwen *et al.* 1998a). These plumes do not mark the vent for the silicate lavas and seem to be the result of the hot lavas volatilizing the SO_2-rich substrate (Kieffer *et al* 2000, Milazzo *et al.* 2001). The chemistry of Prometheus-type plumes should not be used to model conditions in Io's interior (cf. Zolotov and Fegley 1999). In contrast, bright red material deposited by plumes such as Pele mark the location of primary vents for silicate lavas, as inferred from high-resolution images and temperature maps. High-resolution images have shown that plume vent regions include lava flows, lava lakes, and fissures, but we have yet to identify an actual vent construct.

The very late orbits of *Galileo* (G29–I32) revealed a surprise: four large active plumes in the north polar region, confirming the existence of a class of "Pele-type" plumes with red deposits (McEwen and Soderblom 1983) and revealing a new very large plume with bright white deposits. When *Voyager 2* imaged Io four months after *Voyager 1* there were two new 1200-km diameter red plume deposits (Surt and Aten), similar to the deposits of Pele. These two new plume vents were at relatively high latitudes (45° N and 48° S) whereas the others were more equatorial. From the joint *Galileo–Cassini* observations within a few days of 1 January 2001 we were surprised to see a giant new plume (~400 km high) over Tvashtar Catena (63° N) with UV color properties and a 1200-km diameter red plume deposit, both properties very similar to those of Pele (Porco *et al.* 2003). In the I31 flyby (August 2001) *Galileo* flew through the region occupied by the Tvashtar plume seven months earlier. Imaging did not detect a plume, but SO_2 may have been detected by the plasma science experiment (Frank *et al.* 2001). However, the SSI images did reveal a giant (~500 km high) bright plume over the location of a new hot spot detected by NIMS (41° N, 133° W) where no plume had been previously detected, and with a bright white plume deposit (Figure 14.2e). This is reminiscent of a short-lived stage of one of the Loki plumes in 1979, when it reached a height of ~400 km (McEwen *et al.* 1989). The I31 images also revealed a new red ring (1000 km diameter) surrounding Dazhbog Patera (55° N, 302° W) and color/albedo changes suggesting new activity at Surt (Figure 14.2e). An IR outburst with a 1470 K temperature was detected at Surt six months earlier (Marchis *et al.* 2002). Surt, Aten, Tvashtar, and Dazhbog form a class of short-lived Pele-like plumes at high latitudes, but Pele itself is unique because the plume and associated hot spot are very long-lived, active throughout the *Galileo* era (1996–2001).

Possible thermodynamic conditions for Ionian plumes were described by Kieffer (1982). These conditions range from unusually cold to unusually warm as compared to terrestrial volcanism. The coldest reasonable volcanism on Io resembles geyser volcanism on the Earth (liquid SO_2, temperatures below the liquidus of sulfur, 393 K). Liquid SO_2 in a shallow reservoir begins ascending due to buoyancy, and starts boiling at higher levels in the crust. As it erupts, a plume of vapor and ice-condensate forms as the fluid emerges into the cold, low-pressure atmosphere of Io. At slightly higher temperatures on the liquidus of sulfur, the SO_2 boils in the reservoir and upon ascent. This fluid also forms a mixture of vapor and ice in the plume. Finally, either SO_2 or S can exist in superheated vapor states whose temperature is determined by the proximity of silicate magma. Temperatures as high as 2000 K may be present. We would expect such plumes to entrain silicate pyroclastics, consistent with the dark deposits seen around Pele, Pillan, Tvashtar, and other locations.

All-vapor plumes are possible and would be difficult to detect via scattered light; they have been called "stealth plumes" (Johnson *et al.* 1995). The best candidate for a "stealth" SO_2 gas plume detectable only from excited emissions in eclipse was seen over Acala Fluctus (McEwen *et al.* 1998a). Tvashtar may have had a stealth plume during I31, with SO_2 detected by the plasma wave experiment (Frank *et al.* 2001), while no plume was visible to SSI.

Early models for volcanism on Io (Cook *et al.* 1979, Kieffer 1982, Strom and Schneider 1982) considered transformation of thermal energy to velocity to plume height. These models suggested that some plume shapes – those that are relatively symmetric umbrellas, such as Prometheus – could be explained by ballistic-trajectory models (Strom and Schneider 1982, Glaze and Baloga 2000), whereas others probably reflected complex pressure conditions and/or vent geometries. More recently, numerical models of the plume dynamics have been initiated (Zhang *et al.* 2002, Smythe *et al.* 2002). Several phenomena revealed by the simulations were not apparent in the earlier models. For example, eruptions with low (1%) volatile content can form pyroclastic flows (Smythe *et al.* 2002). This raises the possibility that some of the layered plains seen around paterae on Io may be ignimbrites (welded ash flows).

14.3.3 Sulfur Flows

The suggestion that sulfur volcanism may be widespread on Io stemmed from *Voyager*-era observations showing surface colors suggestive of various sulfur allotropes (reviewed by Nash *et al.* 1986). Later observations revealed widespread volcanism at temperatures too high to be consistent with sulfur, but secondary sulfur flows (driven by silicate magmatism) may be common. *Galileo* images show that several percent of Io's surface is covered by especially bright flows that are relatively young (superimposed over their surroundings; see Figures 14.1, 14.2f). There do appear to be older silicate flows with patchy sulfurous fumarolic deposits such as Lei Kung Fluctus (Geissler *et al.* 1999), but the bright young flows have a distinctive appearance and could be composed of sulfur (Williams *et al.* 2002).

Sulfur as secondary volcanism – that is, melting and re-mobilization of sulfur deposits by the injection of hot silicates from below – is a process that occurs on Earth. A particularly good example is the Mauna Loa sulfur flow (Skinner 1970, Greeley *et al.* 1984). Skinner proposed that fumarolic sulfur deposits that had accumulated on the flank of a cone were mobilized by the heat generated by the 1950 eruption of Mauna Loa. *Galileo* data has shown that most dark areas within calderas are associated with silicate volcanism (e.g., McEwen *et al.* 1997, Geissler *et al.* 1999, Lopes-Gautier *et al.* 1999) but bright deposits on paterae floors remain candidate sites of secondary sulfur volcanism. Ra Patera flows were proposed to be sulfur on the basis of *Voyager* image colors (Pieri *et al.* 1984), and subsequent eruptions at Ra in the early 1990s – without the detection of a hot spot – were also consistent with sulfur volcanism (Spencer *et al.* 1997a). Another candidate site is Emakong Patera (Figure 14.5), where high-resolution images show dark, sinuous lava channels or tubes feeding bright, white to yellow flows on areas surrounding the patera. Williams *et al.* (2001b) proposed that these are sulfur flows and showed on the basis of numerical modeling that the flows could have been emplaced in a turbulent regime, consistent with predictions by Sagan (1979) and Fink *et al.* (1983). Repeated observations of Emakong Patera by NIMS consistently showed temperatures below 400 K, thus leaving open the question of whether the erupting material is silicate or sulfur (Lopes *et al.* 2002). The bright white deposits inside Baldur Patera (Figure 14.2f) and elsewhere may be examples of SO_2 flows (Smythe *et al.* 2001).

14.4 RESURFACING RATE AND AGE OF THE SURFACE AND LITHOSPHERE

In spite of high-resolution imaging by *Galileo*, there is not a single convincing example of an impact crater on Io. There are circular craters, but without ejecta blankets, central peaks, or other morphologies typical of fresh impact craters, so it seems likely that these craters are of endogenic origin. Assuming a lunar impact rate and size–frequency distribution, Johnson and Soderblom (1982) showed that all craters are easily erased in 10^6 years with a resurfacing rate $\geq$0.1 cm yr^{-1}.

These estimates can be updated with newer information. Resurfacing of Io (by mass and volume) is probably dominated by lava flows (Phillips 2000). Reynolds *et al.* (1980) showed that the global heat flow can be equated to a resurfacing rate by lavas. The best estimate of heat flow ($\sim$2 W m^{-2}, see below) leads to a global average resurfacing rate of 1.06 cm yr^{-1} by basalt or 0.55 cm yr^{-1} by Commondale komatiites, which Williams *et al.* (2000) considered the best terrestrial analog for high temperature Mg-rich lavas on Io.

The work of Zahnle *et al.* (2003) indicates that a 20-km or larger crater should form on Io every $\sim$3 Myr on average. We expect the combined *Voyager–Galileo* imaging of Io is sufficient to identify the impact origin of a 20-km crater over at least 80% of Io's surface (imaged at 3.2 km/pixel or better). A half-buried crater may or may not be distinguishable from the many paterae on Io, so let's assume 3/4 burial is needed to hide the impact origin of a crater. Assuming a depth:diameter ratio for complex craters like the Moon of 1.3:10 (Pike 1980), about 2 km of fill would be needed to disguise the origin of a 20-km crater. The lack of visible 20-km diameter impact craters indicates >0.05 cm yr^{-1} of resurfacing, if the Zahnle *et al.* (2003) flux is correct. At the current 0.55–1.06 cm yr^{-1} globally averaged lava resurfacing rate, 189 000–364 000 years are required to disguise all 20-km impact craters. Alternatively, if large impacts stimulate local volcanic activity, they may be disguised much more rapidly. If the lithosphere is 50 km thick, then it represents 4.7 to 9.1 $\times$ 10^6 years of volcanic activity (if the resurfacing rate has been constant and spatially uniform), and there should be $\sim$2 impact craters 20 km in diameter or larger buried somewhere in the lithosphere.

What can we say about the variation of resurfacing rates on Io? Based on color/albedo changes (McEwen *et al.* 1998a, Geissler *et al.* 1999b, Phillips 2000) it seems likely that the upper few mm are modified on timescales of centuries or less, but the lava resurfacing rate is more important for understanding the lithosphere. On the timescale of a few years, the resurfacing by lava is highly concentrated on to a few percent of the surface (Phillips 2000). A key issue is whether or not resurfacing is globally uniform over timescales comparable to the age of the lithosphere (a few Myr). *Galileo* returned much higher-resolution images than *Voyager*, and with a lunar-like size–frequency distribution we would expect several hundred times as many craters to be resolvable at 100 m/pixel than at 1 km/pixel resolution.

However, small craters on Europa suggest fewer small primary impactors than expected from assuming that primaries dominate the size–frequency distribution at the Moon (Bierhaus *et al.* 2001). If we assume that the number of craters from 20 to 2 km diameter is proportional to D^{-2}, then we should expect a crater 2 km diameter or larger every 27 000 years, or every 270 000 years over 10% of Io's surface. *Galileo* has imaged ~10% of Io's surface at better than 0.5 km/pixel, sufficient to identify a 2-km crater. The fact that no impact craters have been detected suggests that regions of Io with <0.07 cm yr^{-1} resurfacing by lava over timescales of 10^6 years are uncommon. See Chapter 18 for age estimates for Io based on slightly different assumptions, but with similar results.

14.5 TECTONISM AND MASS WASTING

14.5.1 Paterae

The most common structures on Io are paterae, quasi-circular to polygonal depressions, often associated with especially bright, dark, or colorful deposits (see Figures 14.2, 14.3, 14.5). At least 400 paterae have been mapped, with an average size of ~40 km diameter and peak sizes >200 km; they are up to 3 km deep (Radebaugh *et al.* 2001). They are usually assumed to be volcanic calderas, which form by collapse over shallow magma chambers following partial evacuation. In some ways they resemble large basaltic calderas, which form over shield volcanoes. However, the angular shapes and alignments of many paterae (Williams *et al.* 2002; Figure 14.2f) suggest strong structural control, and most paterae lie on flat plains, with no hint of a shield volcano. Some may not be volcanic calderas in the terrestrial sense but rather structural depressions that were subsequently exploited by magma (e.g., Gish-Bar and Hi'iaka paterae, Figure 14.5). But many paterae are centered on extensive flow fields and are probably primarily volcanic structures, and shallow magma chambers are expected to be common in Io's lithosphere (Leone and Wilson 2001). Perhaps the best terrestrial analog is the volcano-tectonic depression, defined as a caldera-like topographic low that has both volcanic and regional tectonic elements; the extent to which each process has played a role in the formation of the feature is variable (Jackson 1997).

14.5.2 Mountains

The other major structural landforms on Io are the prominent mountains towering over the flat volcanic plains (Figures 14.5, 14.6). *Voyager* and *Galileo* observations provide a near-global inventory of mountains (~85% of the surface). At least 115 mountains covering ~3% of the surface have now been identified and characterized (Carr *et al.* 1998, Schenk *et al.* 2001, Jaeger *et al.* 2003). (We define a mountain as a steep-sided landform rising more than ~1 km above the plains.) Mountains average ~6 km in elevation and range from a few 10s to more than 500 km at their bases. The highest mountain, southern Boosaule Montes, rises ~17 km; the next highest is 13 km high. Most mountains rise abruptly from the plains, but many are partly or completely surrounded by debris aprons, plateaus, and layered plains. Mountains come in a variety of shapes, from flat tabular mesas to sharp angular peaks to asymmetric flatirons to complex rugged massifs.

Dense surface striations are common on mountains. Examples include orthogonal sets of striations on Haemus Montes, and lengthwise oriented striations on Tohil Mons (Figure 14.6). High-resolution *Galileo* views do not reveal if striations are exposed layering or closely spaced fracture planes. Parallel ridges also mark the surfaces of some mountains. Ridges can be oriented down-slope, or across the dominant slope direction (Schenk and Bulmer 1998, Turtle *et al.* 2001, Moore *et al.* 2001). Landslides are common, and mountains generally appear unstable and short-lived, which requires that they be uplifted at a rate comparable to that of their destruction and burial by lava flows. Average mountain uplift rates must exceed the globally averaged resurfacing rate.

The origin(s) of mountains were widely debated post-*Voyager* as they do not appear to be volcanoes and they do not form any global tectonic pattern. Various extensional and compressional models have been proposed to explain mountain formation (Turtle *et al.* 2001, Schenk *et al.* 2001). Compressional uplift probably dominates because the asymmetric shapes suggest the uplift and rotation of crustal blocks (Smith *et al.* 1979, Schenk and Bulmer 1998, Carr *et al.* 1998) and because extension is unlikely to uplift blocks of crust by 10–17 km. Schenk and Bulmer (1998) linked mountain formation directly to the high rate of volcanic resurfacing and implied radially directed recycling of the crust. The radially descending crust shrinks in radius and volume, throwing it into compression, which must be relieved either ductily (i.e., by folding and shortening) or brittly (i.e., by thrust faulting). Since the resurfacing rate is fast compared with the rate of heat conduction, the lithosphere is expected to be cold and brittle (O'Reilly and Davies 1980), so thrust faulting probably dominates. Schenk and Bulmer further suggested that local controls, such as preexisting faults or crustal anisotropies, are needed to explain the apparently random distribution of mountains. Turtle *et al.* (2001) quantitatively tested several mountain formation models and also found that local triggering mechanisms, such as mantle upwelling or downwelling, are required to explain the mountain distribution.

In a variation on the compressive theme, McKinnon *et al.* (2001) proposed that Io's crust is inherently unstable if volcanism on Io is episodic on regional scales. By the heat pipe model of O'Reilly and Davies (1980) (see also Monnereau and Dubuffet 2002), most of Io's heat is lost through volcanic conduits and the crust is relatively cold due to rapid vertical recycling. A slow-down in volcanism would lead to increased heating of the base of the crust and the associated thermal expansion could increase horizontal compressive loads sufficiently to fracture the crust and trigger thrust faulting. Jaeger *et al.* (2003) estimated the stresses based on these two compressional models and concluded that while both are significant, radial subsidence would dominate if the crust is thicker than ~10 km. The thermal expansion could be a significant contributor to compressive stresses only if a major drop in resurfacing rate is sustained for nearly 100 000 years.

14.5.3 Paterae and Mountains: Distributions and Relationships

The absence of any obvious global tectonic pattern among either volcanoes or mountains on Io suggests that any surface expression of internal dynamics (i.e., convection) must be subtle. Indeed, the global inventory of mountains reveals modest nonuniformities in their relative areal density (Schenk *et al.* 2001), with the greatest frequency of mountain occurrence in two large antipodal regions near the equator at 65° W and 265° W. A similar bimodal pattern is also evident in the global distribution of volcanic centers (Schenk *et al.* 2001) and paterae (Radebaugh *et al.* 2001) but offset roughly 90° in longitude, and thus anti-correlated from mountainous regions. These broadly defined centers are offset roughly 30° east of the current tidal axes.

The bimodal distribution pattern for volcanic centers matches the expected pattern of heat flow from asthenospheric tidal heating (Ross *et al.* 1990) and the internal convection pattern within Io's mantle predicted from 3-D simulations (Tackley *et al.* 2001). However, the regional anti-correlation of mountains and volcanic centers is counterintuitive if volcanic resurfacing causes mountain formation. Several hypotheses to explain the regional pattern were presented by Schenk *et al.* (2001): (i) Mountains are shorter-lived in regions of more active resurfacing due to more rapid burial or collapse. (ii) Tall (and longer-lived) mountains form less frequently in regions of higher heat flow and a thinner lithosphere. (iii) An additional stress mechanism is superimposed on the global compressive stresses. Three possibilities have been suggested in case (iii): (1) stresses induced on the lower crust by rising and downwelling mantle convection plumes, (2) nonsynchronous rotation of Io's lithosphere with respect to the interior (Schenk *et al.* 2001, Radebaugh *et al.* 2001), and (3) the model of McKinnon *et al.* (2001). These mechanisms could reduce compressional stresses near the anti- and sub-jovian regions, enhancing volcanism and discouraging mountain formation.

Despite the global scale anti-correlation, individual mountains and volcanoes appear structurally linked in many cases (Figures 14.5, 14.6). Paterae have been identified on or near the flanks of numerous mountains (~40%) and there is a statistically significant spatial association between mountains and volcanic centers (Turtle *et al.* 2001, Jaeger *et al.* 2003). Some mountains directly connect and form apparent structural links between two paterae. Some mountains may have formed along faults radiating from volcanic centers (Schenk and Bulmer 1998). Mountains could also form over small-scale mantle upwellings, consistent with the isolated occurrence of mountains (Jaeger *et al.* 2003). Several mountains show evidence of axial rifting possibly due to uplift-related extension. Fault-bounded mountains could provide ready conduits for migrating lavas in the upper crust. If the global subsidence model for mountain formation is correct, it may be difficult for magmas to ascend to the surface through the compressively stressed lower crust. The formation of thrust faults may locally relieve compressive stresses, sufficient for magmas to ascend. The resulting volcanism may then contribute to the ultimate destruction of the original mountain, for example at Tohil Mons(Schenk *et al.* 2001; Figure 14.6). On the other hand, the majority of mountains are not located near obvious volcanic centers, and their formation may be independent of nearby volcanism.

14.5.4 Mass Wasting

As befits a planet with locally high relief, Io exhibits several styles of mass wasting. Slumping of km-scale blocks and large-scale landslides have been noted in several cases (Schenk and Bulmer 1998, Moore *et al.* 2001), leading to suggestions of failure along weak horizons within the crust. Incoherent slump deposits are found along the flanks of numerous mountains (McEwen *et al.* 2000a, Turtle *et al.* 2001), suggesting simple slope failure. Parallel ridges on mountains (e.g., Hi'iaka Mons, Figure 14.5) have been attributed to down-slope flow or creep of surface layers. Very high-resolution images from I32 show evidence of terracing along the edges of at least one of these tabular plains, indicating the undermining of scarps and subsequent slope failure of the upper layers. Curvilinear scarps 100s of km long (Figures 14.5, 14.6), forming large isolated tabular plains up to 1 km high, are generally interpreted as due to extensive scarp retreat, and in higher resolution images, these scarps can appear to be "choked" by debris. McCauley *et al.* (1979) proposed that local venting of SO_2 could explain the scarp retreat and diffuse bright deposits along many scarps, and this remains an attractive model given the ubiquity of SO_2 and hot spots as confirmed by *Galileo*. Several other mass wasting mechanisms can be envisioned, including plastic flow of interstitial volatiles, sublimation degradation, or disaggregation from chemical decomposition (Moore *et al.* 2001).

14.6 IO'S HEAT FLOW

Io is unique among solid bodies in the solar system in that its heat flow is so high that it can be determined by remote sensing of surface temperatures. Understanding Io's heat flow is important for constraining tidal heating models (see Chapter 13), and for probing Io's interior structure. The discrete volcanic hot spots account for most of the heat flow, but conducted heat from extensive cooling lava flows may also be significant (Stevenson and McNamara 1988). At these longer wavelengths, however, thermal emission from the non-volcanic regions, which are warmed by sunlight, and from absorbed sunlight re-radiated by the hot spots themselves, are also important. This "passive" component must be removed to isolate the hot spot contribution.

Disk-integrated ground-based observations of Io's thermal emission provide uniform longitudinal coverage and a long time base, allowing study of the spatial and temporal variability of the heat flow. Models of the passive component can be constrained by wavelength-dependent changes in Io's thermal emission during Jupiter eclipses (Sinton and Kaminski 1988, Veeder *et al.* 1994). Very rapid initial cooling indicates extensive surface coverage by an extremely insulating, porous, material, such as pyroclastic deposits, that is best modeled as having relatively low albedo. Cooling during the remainder of the eclipse is much slower, due to a combination of a higher thermal inertia, higher-albedo passive component, and emission from volcanic hot spots. As pointed out by Veeder *et al.* (1994), low-temperature hot

spots will be warmed significantly by the Sun, and thus will also cool at night.

Synthesizing their 10 years of ground-based 5–20 micron photometry of Io, Veeder *et al.* (1994) obtained the most comprehensive picture so far of Io's heat flow and its variability. In addition to eclipse cooling, they constrained passive temperatures using *Voyager* estimates of Io's bolometric albedo (Simonelli and Veverka 1988) and *Voyager* infrared observations of Io's nightside temperature (Pearl and Sinton 1982, McEwen *et al.* 1996). They concluded that much of Io's heat flow was radiated from large areas at $T <$ 200 K, little warmer than the passively-heated surface, and that Io's average heat flow is more than 2.5 W m^{-2}, with only modest temporal or spatial variability. They considered their estimate to be a lower limit because the ground-based data are not very sensitive to radiation from high-latitude anomalies, and because they did not include the possible contribution from heat conducted through Io's lithosphere. However, it is possible that rapid downward motion of the crustal materials due to resurfacing (O'Reilly and Davies 1981, Carr *et al.* 1998) minimizes heat conduction through the lithosphere.

Voyager IRIS observations of Io (Pearl and Sinton 1982, McEwen *et al.* 1996), covering the 5–50 micron region, provide an independent measure of heat flow. Here the typical spatial resolution of a few 100 km is sufficient to resolve individual hot spots, and good spectral resolution allows some separation of passive and endogenic radiation within each field of view, by fitting multiple blackbodies to each spectrum and assuming that the lowest-temperature contribution is passive. However, the data do not provide globally homogeneous coverage. Extrapolating from the Jupiter-facing hemisphere, where coverage is best, and assuming that Loki, which radiates more heat than any other Io hot spot, is unique, McEwen *et al.* (1996) estimated a minimum global heat flow of 1.85 W m^{-2}, with likely additional contributions from conducted heat and widespread low-temperature hot spots.

Endogenic emission is more readily separated from passive emission at night, when the passive component is minimized. *Voyager* IRIS obtained sporadic nighttime coverage of Io, but the first hemispheric maps of broadband nighttime emission came from *Galileo* PPR (Spencer *et al.* 2000b). Nighttime temperatures away from the obvious hot spots are near 95 K, and are remarkably independent of both latitude and local time. Making the assumption that at low latitudes this temperature is entirely due to passive emission, that the passive component temperature varies as $\cos^{1/4}$(latitude), and that all emission at higher temperatures is endogenic, Spencer *et al.* (2000b) estimated global heat flow to be 1.7 W m^{-2}, again assuming that Loki was unique. The lack of fall-off in temperature with latitude would then imply excess endogenic emission at high latitudes.

Matson *et al.* (2001) explored the possibility that the uniform nighttime background temperatures were instead due entirely to endogenic heat, with negligible contribution from re-radiated sunlight, and derived a very large upper limit to Io's heat flow of 13.5 W m^{-2}. Spencer *et al.* (2002a) noted, however, that such a large heat flow is readily ruled out by using heat balance considerations. They subtracted the total power of sunlight absorbed by Io (estimated using new bolometric albedo maps by Simonelli *et al.* 2001), from Io's total radiated power, estimated using disk-integrated *Voyager* IRIS spectra of the day and night hemispheres, supplemented by ground-based observations of Io's daytime emission from Veeder *et al.* (1994) and PPR observations of Io's nighttime emission from Spencer *et al.* (2000b). Assuming that Io's emission depends only on phase angle, they obtained a total heat flow of 2.2 ± 0.9 W m^{-2}. Accounting for the likely lower emission at high latitudes than at the equator, and refining error estimates reduces the estimated heat flow to 2.1 ± 0.7 W m^{-2} (J.R. Spencer *et al.* manuscript in preparation; Figure 14.8). (This result is remarkably similar to the very first estimate of Io's heat flow of 2 ± 1 W m^{-2} by Matson *et al.* 1981). Though this technique is not precise, as it involves subtraction of similar-sized quantities known with limited accuracy, it is robust in that the answer does not depend on assumptions about the temperature of the thermal anomalies or how the emission in any particular observation is divided between endogenic and passive components. It also accounts for any heat that is conducted through the lithosphere, and thus provides an actual estimate of, rather than a lower limit to, Io's heat flow. This heat flow estimate is consistent with previous lower limits to the heat flow (i.e., that from hot spots), and indicates that hot spots account for most of Io's heat flow. Thus, the thermal observations support the O'Reilly and Davies (1980) model for volcanic heat advection through a cold lithosphere.

Several lines of evidence indicate that Io's current heat flow and tidal heating rate exceed the long-term equilibrium value. First, Io's current heat flow is about twice as large as the upper limit of ~0.8 W m^{-2} expected for steady-state tidal heating models over 4.5 Ga (Peale 1999); the discrepancy can no longer be considered potentially resolvable from uncertainties in the heat flow estimate, as suggested by Showman and Malhotra (1999). If the theoretical estimates of steady-state heat flow are correct, then Io's heat flow has varied over time due to its orbital evolution. Second, recent secular orbital accelerations suggest that Io is now spiraling slowly inward, losing more energy from internal dissipation than it gains from Jupiter's tidal torque (Aksnes and Franklin 2001). Third, if Io's thermal history varies strongly with time, then the absence of core convection driving a self-sustained magnetic field requires that the mantle be relatively hot (Wienbruch and Spohn 1995). The time-variable thermal/orbital interaction has implications for the geologic histories and futures of Europa and Ganymede as well as Io.

14.7 DISCUSSION: THE LITHOSPHERE AND MANTLE OF IO

Post-*Voyager* models of Io's crust had a rugged differentiated silicate crust mostly covered by layers of silicate and sulfur (molten at depth), and showed the mountains to be ancient protuberances of the silicate subcrust (Schaber 1982, Kieffer 1982, Nash *et al.* 1986). An updated vision of Io's crust and lithosphere (Figure 14.9) is a layered stack of mafic lava flows, interbedded with smaller amounts of silicate and sulfurous pyroclastics, sulfur flows, and volatile species such as SO_2. The mechanical lithosphere in this case corresponds very closely to the crust, which may have relatively minor compositional distinctions from the mantle (i.e., compared with Earth). This lithosphere may be broken into slabs no

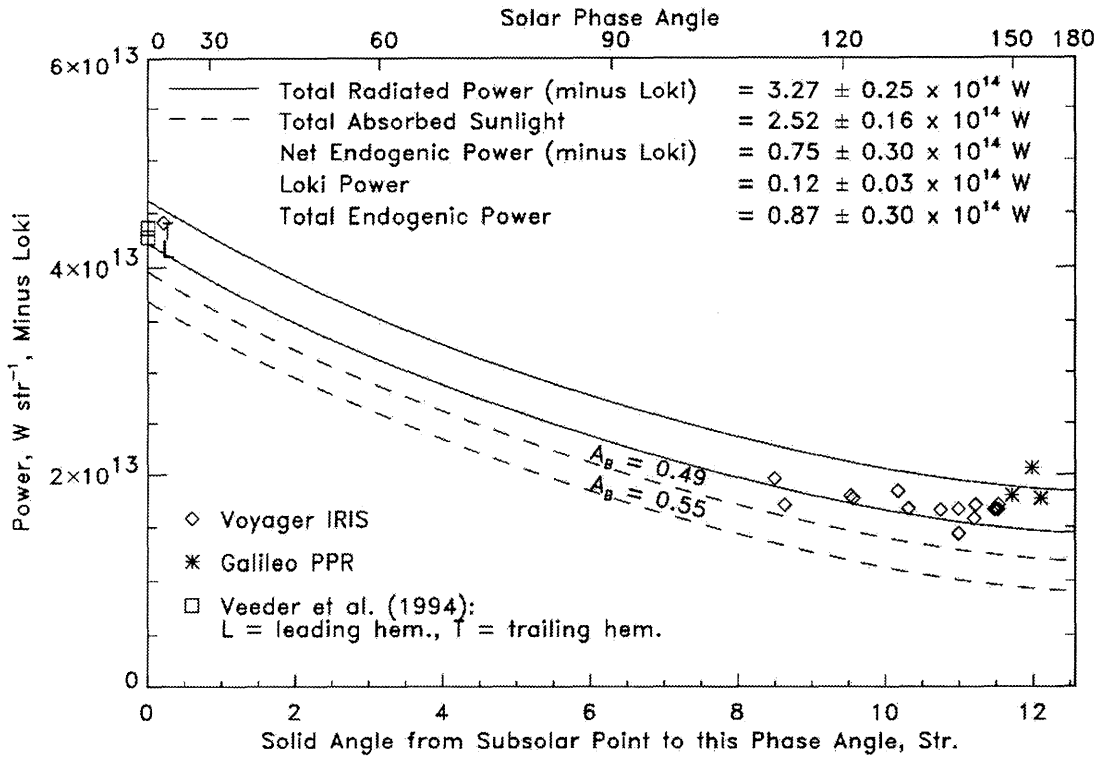

Figure 14.8. Io's disk- and wavelength-integrated thermal emission, measured at low sub-observer latitudes, as a function of phase angle, from various sources (modified from Spencer *et al.* 2002). The upper x-axis scale is solar phase angle (degrees) and the lower x-axis scale is solid angle from the sub-solar point to the corresponding phase angle. The x axis is linear in solid angle, so that the area under curves on the plot represents the total power emitted, after a few percent correction to account for the likely lower emission at high latitudes. The solid curves show plausible upper- and lower-bound fits to the data, and the dashed curves show expected passive thermal emission for the bolometric albedo range 0.52 +/−0.03. Also shown is the range of powers corresponding to these curves, and the resulting net endogenic power.

smaller than a few hundred kilometers judging by the typical dimensions of the massifs. Occasional lithospheric blocks are upthrust along deep-rooted thrust faults to form mountains. Punctuating this broken layered stack are hundreds of volcanic conduits or magma chambers, some of which may feed dikes or sills intruded along existing faults, along horizontal bedding planes or elsewhere. This lithosphere is relatively cold and isothermal (O'Reilly and Davies 1980, Carr *et al.* 1998) except near the base where the thermal gradient must be very steep. The thermal gradient may also be steep under caldera floors, if they reside over shallow magma chambers.

There is still no consensus on the average thickness of Io's lithosphere, except that it must exceed ~15 km. Carr *et al.* (1998) gave an example where the depth of isostatic compensation would be ~90 km, but wrote "The mountains may, however, be uncompensated and partially supported by a thick rigid lithosphere. Even so, it is difficult to see how 10 km high mountains could be supported by a mechanical lithosphere that is less than 30 km thick, particularly since there is no evidence of moats having formed around the mountains as a result of flexure of the lithosphere..." McKinnon *et al.* (2001) presented a crustal chaos hypothesis and wrote "Mountain lengths range from ~50 to >400 km, and the crustal thickness is probably some sizeable fraction of this, perhaps as great as 25–100 km." Jaeger *et al.*

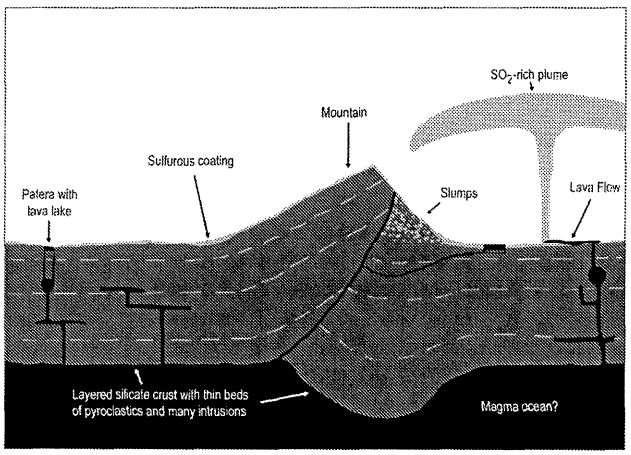

Figure 14.9. Cartoon of Io's crust. The Ionian crust is thought to be dominated by layers of mafic silicate lava flows with thin beds of sulfurous and silicate pyroclastic deposits. A sulfur dioxide-rich coating blankets most of the surface away from hot spots. Prometheus-type plumes are generally caused by lavas advancing over this volatile blanket. Plumes of primary volcanic gas are most visible at UV wavelengths and are not illustrated here. Mountains are formed by deep thrust faults and the crust is underlain by a zone with significant melting, perhaps a magma ocean.

(2003) conclude that a minimum lithospheric thickness of 14 km is required to provide sufficient compressive stress to explain the existing mountains, and Schenk *et al.* (2001) pointed out that the lithosphere must be at least as thick as the tallest mountains (13–17 km) if they are thrusted blocks. The lithosphere may vary in thickness; perhaps it is thicker in regions where mountains are concentrated (Schenk *et al.* 2001) and in the polar regions (McEwen *et al.* 2000a).

The cold subsiding lithosphere model, combined with new observational data, has important implications for the chemical composition of the crust and the physical state of the mantle of Io. The predicted temperature profile requires that the crust/mantle boundary and the lithosphere/asthenosphere boundary coincide to within a few kilometers. If Io is predominantly solid, then the lava seen at the surface must originate in a partially molten mantle. These lavas are subjected to repeated episodes of partial melting when they are buried to the depth of the zone of melting. Each episode of partial melting will chemically distil the rocks, producing a buoyant liquid enriched in incompatible elements (e.g., Na, K, Si, H) and a dense solid residue enriched in compatible elements (e.g., Mg). If Io underwent the current level of volcanic activity for even a fraction of the age of the solar system, the entire silicate portion of Io should have gone through hundreds of episodes of partial melting. This would produce extreme differentiation of the rock types through the crust and mantle. While processes such as assimilation of wall rocks during ascent of magma would cause some mixing, one would expect Io to have a wide variety of silicate lava types. Furthermore, the compositions should be dominated by the most easily melted (i.e., lowest melting temperature) lavas (Keszthelyi and McEwen 1997). It would be difficult for dense mafic melts from the mantle to rise through the low-density crust and reach the surface.

Instead, the observations of temperatures, colors, and landforms suggest that Ionian volcanism is dominated by mafic lavas. This requires that the crust be very efficiently mixed back into the mantle to erase the distillation effects of partial melting (Carr *et al.* 1998). The simplest way to achieve this level of mixing is if the top of the mantle is molten, leading to rapid and efficient mechanical and chemical mixing. Since such mixing must take place across the globe of Io, it suggests a global layer of melt (Keszthelyi *et al.* 1999). Theoretical studies have shown that there cannot be a global layer of pure liquid magma under the Ionian lithosphere because this would not produce the observed tidal heat flux (e.g., Schubert *et al.* 1981, Ojakangas and Stevenson 1986). However, a crystal-rich magma ocean is allowed by these studies. Using a petrologic model (Ghiorso and Sack 1995) and a dry chondritic bulk composition for Io, the magma ocean is predicted to go from ~60% melt at the base of the lithosphere to only ~5% melt at the core–mantle boundary (Keszthelyi *et al.* 1999). A magma ocean is not required to remove Io's heat (Moore 2001) but may be required to prevent the formation of a low-density crust that would be a significant barrier to mafic volcanism.

The observations to date are all consistent with the idea of a partially crystalline global magma ocean, but may not discriminate this model from rapid solid-state convection (Schubert *et al.* Chapter 13). As predicted by the magma ocean model (Spohn 1997), Io has no intrinsic magnetic field (Kivelson *et al.* Chapter 21). The high temperature of the magma ocean would lead to a stably stratified liquid iron core within Io. However, the lack of magnetic field is not proof of a magma ocean within Io.

The distribution of volcanism on the surface of Io provides some additional, inconclusive, clues about the state of the interior. Segatz *et al.* (1988) calculated that if tidal heating is predominantly at the base of the mantle, heat generation should be concentrated at the poles. Conversely, if heat is mostly generated at the top of the mantle, heat flow will be highest along the equator. The distribution of persistent hot spots (Lopes-Gautier *et al.* 1999), volcanic centers (Schenk *et al.* 2001) and paterae (Radebaugh *et al.* 2001) are concentrated in a manner consistent with tidal heating mostly in the upper mantle. However, the more sporadic but highly energetic volcanic eruptions seen at high latitudes and the higher than expected background temperatures require either some heat generation deep within Io's mantle or some mechanism for lateral heat transport within the mantle. A partially molten magma ocean as hypothesized by Keszthelyi *et al.* (1999) could fit these observations, but so could a vigorously convecting solid mantle (Tackley *et al.* 2001).

14.8 FUTURE EXPLORATION

Though our understanding of Io has increased greatly in the past decade, there is much more we can learn from this dynamic world. We can witness large-scale volcanic and tectonic processes on Io that inform us about ancient and modern processes on the terrestrial planets. Perhaps we could directly observe the formation and/or destruction of landforms such as mountains and paterae. Many important questions lack complete answers.

- What was the coupled orbital evolution of Io–Europa–Ganymede and how has it affected the thermal evolution of all three worlds?
- Are tidal heating and core convection periodic?
- Does Io have a magma ocean?
- What are the mantle convection patterns within Io and how does that influence the volcanism and tectonism?
- What is the composition of the crust, and is the crust equivalent to the lithosphere?
- How uniform is the resurfacing over time periods important to the tectonism ($\sim 10^5$–10^6 years)?
- What are the timescales for formation and destruction of mountains and paterae?
- Are there identifiable impact craters on Io?
- What is the composition of the silicate lavas?
- Are the high temperatures due to Mg-rich lava compositions, some other composition, or some mechanism for "superheating" the lava?
- How common are lava temperatures too hot for normal (not superheated) basalt?
- How common are lava lakes, how do they work, and how much do they influence heat loss?
- Is Io's current heat flow typical or anomalous?
- Why are the styles of volcanism different in the polar regions?
- Is the polar heat flow higher or lower than average?
- What are the mechanisms of faulting and tectonics?

- Are there topographic bulges due to mantle plumes and lithospheric thinning?
- Why are mountains and paterae often associated with each other on local scales?
- Why are they anti-correlated on hemispheric scales?
- What is the inventory and distribution of crustal volatiles and how do they affect the geologic processes?
- Are sulfur or SO_2 flows common?
- How do the volatiles affect mass wasting, sapping, and other processes of landscape modification?
- What are the mechanisms driving the various types of plumes?
- What are the sources of sodium, potassium and chlorine escaping from Io?
- Can the volcanic gasses help us to better understand the chemistry of Io's crust and mantle?

There is much we can still learn about Io via observations from the Earth's surface or near-Earth space. The Hubble Space Telescope, and the new class of 8-meter telescopes when coupled with adaptive optics techniques (Marchis *et al.* 2001), can resolve 100-km scale features, allowing location and characterization of volcanic eruptions and studies of compositional changes. The composition and spatial distribution of Io's atmosphere, and its response to volcanism, can be studied at millimeter wavelengths, in the infrared at 20 microns, and from HST in the ultraviolet. A decade or so from now, the next generation of space telescopes with improved spatial resolution and sensitivity is expected to provide many new opportunities for Io studies.

Many advances in our understanding, however, must await a return to Io by a spacecraft with more capable instrumentation and much higher data return capability than *Galileo*. Io's intrinsic interest as the only place beyond Earth where we can watch large-scale geology in action, and its potential to teach us about the fundamental process of tidal heating, makes a return to Io a high priority. A jovicentric orbiter with many Io flybys is probably the most practical mission concept in the near term. Radiation-hard electronics currently under development could allow a spacecraft to survive more than 50 Io flybys, sufficient to sample a wide range of eruptions and other dynamic phenomena. A functioning high-gain antenna and modern high-capacity data recorders would enable 10^5–10^6 times greater data return per flyby than *Galileo*, providing significant coverage at the high spatial, spectral, and temporal resolutions needed to understand dynamic processes. Improved topographic mapping at all scales, especially globally, is needed to test models for the dissipation of tidal heating, internal convection, and tectonics. Penetrators might be practical, allowing seismic studies of the interior; this is the best way to confirm or refute the magma ocean hypothesis. Io studies could be readily combined with studies of the jovian magnetosphere or the other Galilean satellites.

For a detailed discussion of options for future Io exploration, see Spencer *et al.* (2002b). We look forward to future exploration of Io, and to continued progress in our understanding of one of the most spectacular places in the solar system.

Acknowledgements. We thank the *Galileo* flight team for their dedication and we thank several colleagues for helpful reviews.

REFERENCES

Aksnes, K. and F. A. Franklin, Secular acceleration of Io derived from mutual satellite events, *AJ* **122**, 2734–2739, 2001.

Anderson, J. D., R. A. Jacobson, E. L. Lau, W. B. Moore, and G. Schubert, Io's gravity field and interior structure, *J. Geophys. Res.* **106**, 32 963–32 970, 2001.

Bierhaus, E. B., C. R. Chapman, W. J. Merline, S. M. Brooks, and E. Asphaug, Pwyll secondaries and other small craters on Europa, *Icarus* **153**, 264–276, 2001.

Carlson, R. W., W. D. Smythe, R. M. C. Lopes-Gautier, A. G. Davies, L. W. Kamp, J. A. Mosher, L. A. Soderblom, F. E. Leader, R. Mehlman, R. N. Clark, and F. P. Fanale, Distribution of sulfur dioxide and other infrared absorbers on the surface of Io, *Geophys. Res. Lett.* **24**, 2479, 1997.

Carlson, R. W., R. E. Johnson, M. S. Anderson, J. H. Shirley, M. Wong, S. Douté, and B. Schmitt, Radiolytic influence on the surface composition of the Galilean satellites, in *Jupiter: Planet, Satellites, and Magnetosphere*, pp. 22–23, 2001.

Carr, M. H., Silicate volcanism on Io, *J. Geophys. Res.* **91**, 3521–3532, 1986.

Carr, M. H., A. S. McEwen, K. A. Howard, F. C. Chuang, P. Thomas, P. Schuster, J. Oberst, G. Neukum, and G. Schubert, Mountains and calderas on Io: Possible implications for lithosphere structure and magma generation, *Icarus* **135**, 146–165, 1998.

Consolmagno, G. J., Io: Thermal models and chemical evolution, *Icarus* **47**, 36–45, 1981.

Cook, A. F., E. M. Shoemaker, and B. A. Smith, Dynamics of volcanic plumes on Io, *Nature* **280**, 743–746, 1979.

Coustenis, A., T. Encrenaz, E. Lellouch, A. Salama, T. Müller, M. J. Burgdorf, B. Schmitt, H. Feuchtgruber, B. Schulz, S. Ott, T. de Graauw, M. J. Griffin, and M. F. Kessler, Observations of planetary satellites with ISO, *Adv. Space Res.* **30**, 1971–1977, 2002.

Davies, A. G., Io's volcanism: Thermo-physical models of silicate lava compared with observations of thermal emission, *Icarus* **124**, 45–61, 1996.

Davies, A. G., Volcanism on Io: The view from *Galileo*, *Astron. Geophys.* **42**, 2.10–2.15, 2001.

Davies, A. G., R. Lopes-Gautier, W. D. Smythe, and R. W. Carlson, Silicate cooling model fits to *Galileo* NIMS data of volcanism on Io, *Icarus* **148**, 211–225, 2000.

Davies, A. G., L. P. Keszthelyi, D. A. Williams, C. B. Phillips, A. S. McEwen, R. M. C. Lopes, W. D. Smythe, L. W. Kamp, L. A. Soderblom, and R. W. Carlson, Thermal signature, eruption style, and eruption evolution at Pele and Pillan on Io, *J. Geophys. Res.* **106**, 33 079–33 104, 2001.

Douté, S., B. Schmitt, R. Lopes-Gautier, R. Carlson, L. Soderblom, J. Shirley, and the *Galileo* NIMS Team, Mapping SO_2 frost on Io by the modeling of NIMS hyperspectral images, *Icarus* **149**, 107–132, 2001.

Douté, S., R. Lopes, L. W. Kamp, R. Carlson, B. Schmitt, and the *Galileo* NIMS Team, Dynamics and evolution of SO_2 gas condensation around Prometheus-like volcanic plumes on Io as seen by the Near Infrared Mapping Spectrometer, *Icarus* **158**, 460–482, 2002.

Douté, S., P. Geissler, R. Lopes-Gautier, R. Carlson, and the *Galileo* NIMS team, Spatial distribution and chemical nature of the 1.0 micron absorber on Io's surface inferred by the Near Infrared Mapping Spectrometer and the Solid State Imager of *Galileo*, in *Jupiter: Planet, Satellites, and Magnetosphere*, pp. 22–23, 2001.

Erickson, J. K., Z. N. Cox, B. G. Paczkowski, R. W. Sible, and E. E. Theilig, Project *Galileo*: Completing Europa, preparing for Io, *Acta Astronomica* **47**, 419–441, 2000.

Fanale, F. P., R. H. Brown, D. P. Cruikshank, and R. N. Clake, Significance of absorption features in Io's IR reflectance spectrum, *Nature* **280**, 761–763, 1979.

Fanale, F. P., W. B. Banerdt, L. S. Elson, T. V. Johnson, and R. W. Zurek, Io's surface: Its phase composition and influence on Io's atmosphere and Jupiter's magnetosphere, in *Satellites of Jupiter*, D. Morrison (ed), University of Arizona Press, pp. 756–781, 1982.

Fink, J. H., S. O. Park, and R. Greeley, Cooling and deformation of sulfur flows, *Icarus* **56**, 38–50, 1983.

Frank, L. A. and W. R. Paterson, Production of hydrogen ions at Io, *J. Geophys. Res.* **104**, 10 345–10 354, 1999.

Frank, L. A. and W. R. Paterson, Passage through Io's ionospheric plasmas by the *Galileo* spacecraft, *J. Geophys. Res.* **106**, 26 209–26 224, 2001.

Gaskell, R. W., S. P. Synnott, A. S. McEwen, and G. G. Schaber, Large-scale topography of Io: Implications for internal structure and heat transfer, *Geophys. Res. Lett.* **15**, 581–584, 1988.

Geissler, P., A. McEwen, C. Phillips, D. Simonelli, R. M. C. Lopes, and S. Douté, *Galileo* imaging of SO_2 frosts on Io, *J. Geophys. Res.* **106**, 33 253–33 266, 2001.

Geissler, P. E., A. S. McEwen, L. Keszthelyi, R. Lopes-Gautier, J. Granahan, and D. P. Simonelli, Global color variations on Io, *Icarus* **140**, 265–282, 1999.

Ghiorso, M. S. and R. O. Sack, Chemical mass transfer in magmatic processes: IV. A revised and internally consistent thermodynamic model for the interpolation and extrapolation of liquid–solid equilibria in magmatic systems at elevated temperatures and pressure, *Contributions to Mineralogy and Petrology* **119**, 197–212, 1995.

Glaze, L. S. and S. M. Baloga, Stochastic–ballistic eruption plumes on Io, *J. Geophys. Res.* **105**, 17 579–17 588, 2000.

Greeley, R., E. Theilig, and P. Christensen, The Mauna Loa sulfur flow as an analog to secondary sulfur flows on Io, *Icarus* **60**, 189–199, 1984.

Greenberg, R., Orbital evolution of the Galilean satellites, in *Satellites of Jupiter*, D. Morrison (ed), University of Arizona Press, pp. 65–92, 1982.

Hapke, B., The surface of Io: A new model, *Icarus* **79**, 56–74, 1989.

Howell, R. R., Thermal emission from lava flows on Io, *Icarus* **127**, 394–407, 1997.

Howell, R. R., F. P. Fanale, and D. P. Cruikshank, Sulfur dioxide on Io: Spatial distribution and physical state, *Icarus* **57**, 83–92, 1984.

Howell, R. R., J. R. Spencer, J. D. Goguen, F. Marchis, R. Prangé, T. Fusco, D. L. Blaney, G. J. Veeder, J. A. Rathbun, G. S. Orton, A. J. Grocholski, J. A. Stansberry, G. S. Kanner, and E. K. Hege, Ground-based observations of volcanism on Io in 1999 and early 2000, *J. Geophys. Res.* **106**, 33 129–33 140, 2001.

Ingersoll, A. P., Io meteorology: How atmospheric pressure is controlled locally by volcanos and surface frosts, *Icarus* **81**, 298–313, 1989.

Jackson, J. A., ed., *Glossary of Geology*, p. 769, American Geological Institution, 1997.

Jaeger, W. L., E. P. Turtle, L. P. Keszthelyi, J. Radebaugh, A. S. McEwen, and R. T. Pappalardo, Orogenic tectonism on io, *J. Geophys. Res.* **in press**, 2003.

Johnson, R. E., *Energetic Charged-Particle Interactions with Atmospheres and Surfaces*, Springer-Verlag, 1990.

Johnson, R. E. and T. I. Quickenden, Photolysis and radiolysis of water ice on outer solar system bodies, *J. Geophys. Res.* **102**, 10 985–10 996, 1997.

Johnson, T. V. and L. A. Soderblom, Volcanic eruptions on Io: Implications for surface evolution and mass loss, in *Satellites of Jupiter*, D. Morrison (ed), University of Arizona Press, pp. 634–646, 1982.

Johnson, T. V., D. L. Matson, D. L. Blaney, G. J. Veeder, and A. Davies, Stealth plumes on Io, *Geophys. Res. Lett.* **22**, 3293, 1995.

Kargel, J. S., P. Delmelle, and D. B. Nash, Volcanogenic sulfur on Earth and Io: Composition and spectroscopy, *Icarus* **142**, 249–280, 1999.

Keszthelyi, L. and A. McEwen, Magmatic differentiation of Io, *Icarus* **130**, 437–448, 1997.

Keszthelyi, L., A. S. McEwen, and G. J. Taylor, Revisiting the hypothesis of a mushy global magma ocean in Io, *Icarus* **141**, 415–419, 1999.

Keszthelyi, L., A. S. McEwen, C. B. Phillips, M. Milazzo, P. Geissler, E. P. Turtle, J. Radebaugh, D. A. Williams, D. P. Simonelli, H. H. Breneman, K. P. Klaasen, G. Levanas, and T. Denk, *Galileo* SSI Team, Imaging of volcanic activity on Jupiter's moon Io by *Galileo* during the *Galileo* Europa mission and the *Galileo* millennium mission, *J. Geophys. Res.* **106**, 33 025–33 052, 2001.

Khanna, R. K., J. C. Pearl, and R. Dahmani, Infrared spectra and structure of solid phases of sulfur trioxide: Possible identification of solid SO_3 on Io's surface, *Icarus* **115**, 250–257, 1995.

Kieffer, S. W., Dynamics and thermodynamics of volcanic eruptions: Implications for the plumes on Io, in *Satellites of Jupiter*, D. Morrison (ed), University of Arizona Press, pp. 647–723, 1982.

Kieffer, S. W., R. Lopes-Gautier, A. McEwen, W. Smythe, L. Keszthelyi, and R. Carlson, Prometheus: Io's wandering plume, *Science* **288**, 1204–1208, 2000.

Kuskov, O. L. and V. A. Kronrod, Resemblance and difference between the constitution of the Moon and Io, *Planet. Space Sci.* **48**, 717–726, 2000.

Laplace, P. S., *Mécanique Celeste*, vol. 4, (trans. N. Bowditch 1966), 1805.

Lee, S. W. and P. C. Thomas, Near-surface flow of volcanic gases on Io, *Icarus* **44**, 280–290, 1980.

Leone, G. and L. Wilson, Density structure of Io and the migration of magma through its lithosphere, *J. Geophys. Res.* **106**, 32 983–32 996, 2001.

Lopes, R. M. C., L. W. Kamp, S. Douté, W. D. Smythe, R. W. Carlson, A. S. McEwen, P. E. Geissler, S. W. Kieffer, F. E. Leader, A. G. Davies, E. Barbinis, R. Mehlman, M. Segura, J. Shirley, and L. A. Soderblom, Io in the near infrared: Near Infrared Mapping Spectrometer (NIMS) results from the *Galileo* flybys in 1999 and 2000, *J. Geophys. Res.* **106**, 33 053–33 078, 2001.

Lopes, R. M. C., L. W. Kamp, A. G. Davies, W. D. Smythe, R. W. Carlson, S. Douté, A. McEwen, E. P. Turtle, F. Leader, R. Mehlman, J. Shirley, M. Segura, and the *Galileo* NIMS Team, *Galileo*'s last fly-bys of Io: NIMS observations of Loki, Tupan, and Emakong Calderas, in *Lunar and Planetary Science Conference Abstracts*, vol. 33, p. 1793, 2002.

Lopes-Gautier, R., A. S. McEwen, W. B. Smythe, P. E. Geissler, L. Kamp, A. G. Davies, J. R. Spencer, L. Keszthelyi, R. Carlson, F. E. Leader, R. Mehlman, L. Soderblom, and the *Galileo* NIMS and SSI Teams, Active volcanism on Io: Global distribution and variations in activity, *Icarus* **140**, 243–264, 1999.

Lopes-Gautier, R., S. Douté, W. D. Smythe, L. W. Kamp, R. W. Carlson, A. G. Davies, F. E. Leader, A. S. McEwen, P. E. Geissler, S. W. Kieffer, L. Keszthelyi, E. Barbinis, R. Mehlman, M. Segura, J. Shirley, and L. A. Soderblom, A close-up look at Io from *Galileo*'s Near Infrared Mapping Spectrometer, *Science* **288**, 1201–1204, 2000.

Lunine, J. I. and D. J. Stevenson, Physics and chemistry of sulfur lakes on Io, *Icarus* **64**, 345–367, 1985.

Marchis, F., R. Prangé, and T. Fusco, A survey of Io's vocanism by adaptive optics observations in the 3.8-micron thermal band (1996–1999), *J. Geophys. Res.* **106**, 33 141–33 160, 2001.

Marchis, F., I. de Pater, A. Davies, H. Roe, T. Fusco, D. Le Mignant, P. Descamps, B. A. Macintosh, and R. Prangé, High resolution Keck adaptive optics imaging of violent volcanic activity on Io, *Icarus* **160**, 124–131, 2002a.

Marchis, F., I. de Pater, A. G. Davies, H. G. Roe, T. Fusco, D. Le Mignant, P. Descamps, B. A. Macintosh, and R. Prangé, High-resolution Keck adaptive optics imaging of violent volcanic activity on Io, *Icarus* **160**, 124–131, 2002b.

Matson, D. L., G. A. Ransford, and T. V. Johnson, Heat flow from Io/JI, *J. Geophys. Res.* **86**, 1664–1672, 1981.

Matson, D. L., T. V. Johnson, G. J. Veeder, D. L. Blaney, and A. G. Davies, Upper bound on Io's heat flow, *J. Geophys. Res.* **106**, 33 021–33 024, 2001.

McCauley, J. F., L. A. Soderblom, and B. A. Smith, Erosional scarps on Io, *Nature* **280**, 736–738, 1979.

McEwen, A. S. and L. A. Soderblom, Two classes of volcanic plumes on Io, *Icarus* **55**, 191–217, 1983.

McEwen, A. S., L. A. Soderblom, T. V. Johnson, and D. L. Matson, The global distribution, abundance, and stability of SO_2 on Io, *Icarus* **75**, 450–478, 1988.

McEwen, A. S., J. I. Lunine, and M. H. Carr, Dynamic Geophysics of Io, in *Time-Variable Phenomena in the Jovian System.* M. J. S. Belton, R. A. West, J. Rahe (eds), *NASA*, vol. 494, pp. 11–46, 1989.

McEwen, A. S., N. R. Isbell, K. E. Edwards, and J. C. Pearl, Temperatures on Io: Implications to geophysics, volcanology, and volatile transport, in *Lunar and Planetary Science Conference Abstracts*, vol. 27, p. 843, 1996.

McEwen, A. S., D. P. Simonelli, D. R. Senske, K. P. Klaasen, L. Keszthelyi, T. V. Johnson, P. E. Geissler, M. H. Carr, and M. J. S. Belton, High-temperature hot spots on Io as seen by the *Galileo* solid state imaging (SSI) experiment, *Geophys. Res. Lett.* **24**, 2443, 1997.

McEwen, A. S., L. Keszthelyi, P. Geissler, D. P. Simonelli, M. H. Carr, T. V. Johnson, K. P. Klaasen, H. H. Breneman, T. J. Jones, J. M. Kaufman, K. P. Magee, D. A. Senske, M. J. S. Belton, and G. Schubert, Active volcanism on Io as seen by *Galileo* SSI, *Icarus* **135**, 181–219, 1998a.

McEwen, A. S., L. Keszthelyi, J. R. Spencer, G. Schubert, D. L. Matson, R. Lopes-Gautier, K. P. Klaasen, T. V. Johnson, J. W. Head, P. Geissler, S. Fagents, A. G. Davies, M. H. Carr, H. H. Breneman, and M. J. S. Belton, High-temperature silicate volcanism on Jupiter's moon Io, *Science* **281**, 87–90, 1998b.

McEwen, A. S., M. J. S. Belton, H. H. Breneman, S. A. Fagents, P. Geissler, R. Greeley, J. W. Head, G. Hoppa, W. L. Jaeger, T. V. Johnson, L. Keszthelyi, K. P. Klaasen, R. Lopes-Gautier, K. P. Magee, M. P. Milazzo, J. M. Moore, R. T. Pappalardo, C. B. Phillips, J. Radebaugh, G. Schubert, P. Schuster, D. P. Simonelli, R. Sullivan, P. C. Thomas, E. P. Turtle, and D. A. Williams, *Galileo* at Io: Results from high-resolution imaging, *Science* **288**, 1193–1198, 2000a.

McEwen, A. S., R. Lopes-Gautier, L. Keszthelyi, and S. W. Keiffer, Extreme volcanism on Jupiter's moon Io, in *Environmental Effects on Volcanic Eruptions: From Deep Oceans to Deep Space*, pp. 179–205, 2000b.

McKinnon, W., P. Schenk, and A. Dombard, Chaos on Io: A model for formation of mountain blocks by crustal healing, melting and tilting, *Geology* **29**, 103–106, 2001a.

McKinnon, W. B., P. M. Schenk, and A. Dombard, Chaos on Io: A model for formation of mountain blocks by crustal healing, melting and tilting, *Geology* **29**, 103–106, 2001b.

Milazzo, M. P., L. P. Keszthelyi, and A. S. McEwen, Observations and initial modeling of lava: SO_2 interactions at Prometheus, Io, *J. Geophys. Res.* **106**, 33 121–33 128, 2001.

Monnereau, M. and F. Dubuffet, Is Io's mantle really molten?, *Icarus* **158**, 450–459, 2002.

Moore, J. M., R. J. Sullivan, F. C. Chuang, J. W. Head, A. S. McEwen, M. P. Milazzo, B. E. Nixon, R. T. Pappalardo, P. M. Schenk, and E. P. Turtle, Landform degradation and slope processes on Io: The *Galileo* view, *J. Geophys. Res.* **106**, 33 223–33 240, 2001.

Morabito, L. A., S. P. Synnott, P. N. Kupferman, and S. A. Collins, Discovery of currently active extraterrestrial volcanism, *Science* **204**, 972, 1979.

Moses, J. I. and D. B. Nash, Phase transformations and the spectral reflectance of solid sulfur: Can metastable sulfur allotropes exist on Io?, *Icarus* **89**, 277–304, 1991.

Nash, D. B. and R. R. Howell, Hydrogen sulfide on Io: Evidence from telescopic and laboratory infrared spectra, *Science* **244**, 454–457, 1989.

Nash, D. B., F. P. Fanale, and R. M. Nelson, SO_2 frost: UV-visible reflectivity and Io surface coverage, *Geophys. Res. Lett.* **7**, 665–668, 1980.

Nash, D. B., C. F. Yoder, M. H. Carr, J. Gradie, and D. M. Hunten, Io, in *Satellites*, J. A. Burns and M. S. Matthews, eds, pp. 629–688, University of Arizona Press, Tucson, 1986.

Nelson, R. M. and W. D. Smythe, Spectral reflectance of solid sulfur trioxide (0.25–5.2 micron): Implications for Jupiter's satellite Io, *Icarus* **66**, 181–187, 1986.

Nelson, R. M., A. L. Lane, D. L. Matson, F. P. Fanale, D. B. Nash, and T. V. Johnson, Io: Longtudinal distribution of sulfur dioxide frost, *Science* **210**, 784–786, 1980.

Ojakangas, G. W. and D. J. Stevenson, Episodic volcanism of tidally heated satellites with application to Io, *Icarus* **66**, 341–358, 1986.

O'Reilly, T. C. and G. F. Davies, Magma transport of heat on Io: A mechanism allowing a thick lithosphere, *Geophys. Res. Lett.* **8**, 313–316, 1981.

Peale, S. J., P. Cassen, and R. T. Reynolds, Melting of Io by tidal dissipation, *Science* **203**, 892–894, 1979.

Pearl, J., R. Hanel, V. Kunde, W. Maguire, K. Fox, S. Gupta, C. Ponnamperuma, and F. Raulin, Identification of gaseous SO_2 and new upper limits for other gases on Io, *Nature* **280**, 755–758, 1979.

Pearl, J. C. and W. M. Sinton, Hot spots of Io, in *Satellites of Jupiter*, D. Morrison (ed), University of Arizona Press, pp. 724–755, 1982.

Phillips, C. B., *Voyager and Galileo SSI Views of Volcanic Resurfacing on Io and the Search for Geologic Activity on Europa*, Ph.D. thesis, 2000.

Pieri, D. C., R. M. Nelson, S. M. Baloga, and C. Sagan, Sulfur flows of Ra Patera, Io, *Icarus* **60**, 685–700, 1984.

Pike, R. J., Control of crater morphology by gravity and target type: Mars, Earth, Moon, in *Lunar and Planetary Science Conference Abstracts*, vol. 11, pp. 2159–2189, 1980.

Pollack, J. B., F. C. Witteborn, E. F. Erickson, D. W. Strecker, B. J. Baldwin, and T. E. Bunch, Near-infrared spectra of the Galilean satellites: Observations and compositional implications, *Icarus* **36**, 271–303, 1978.

Porco, C. C., R. A. West, A. McEwen, A. D. Del Genio, A. P. Ingersoll, P. Thomas, S. Squyres, L. Dones, C. D. Murray, T. V. Johnson, J. A. Burns, A. Brahic, G. Neukum, J. Veverka, J. M. Barbara, T. Denk, M. Evans, J. J. Ferrier, P. Geissler, P. Helfenstein, T. Roatsch, H. Throop, M. Tiscareno, and A. R. Vasavada, *Cassini* imaging of Jupiter's atmosphere, satellites, and rings, *Science* **299**, 1541–1547, 2003.

Radebaugh, J., L. P. Keszthelyi, A. S. McEwen, E. P. Turtle, W. Jaeger, and M. Milazzo, Paterae on Io: A new type of volcanic caldera?, *J. Geophys. Res.* **106**, 33 005–33 020, 2001.

Rathbun, J. R., J. R. Spencer, L. K. Tamppari, T. Z. Martin, L. Barnard, and L. D. Travis, Mapping of Io's thermal radiation by the *Galileo* Photopolarimeter-Radiometer (PPR) Instrument, *Icarus* **submitted**, 2003.

Reynolds, R. T., P. Cassen, and S. J. Peale, Io: Energy constraints and plume volcanism, *Icarus* **44**, 234–239, 1980.

Ross, M. N., G. Schubert, T. Spohn, and R. W. Gaskell, Internal structure of Io and the global distribution of its topography, *Icarus* **85**, 309–325, 1990.

Russell, C. T. and M. G. Kivelson, Evidence for sulfur dioxide, sulfur monoxide, and hydrogen sulfide in the Io exosphere, *J. Geophys. Res.* **106**, 33 267–33 272, 2001.

Sagan, C., Sulphur flows on Io, *Nature* **280**, 750–753, 1979.

Salama, F., L. J. Allamandola, F. C. Witteborn, D. P. Cruikshank, S. A. Sandford, and J. D. Bregman, The 2.5–5.0 micron spectra of Io: Evidence for H_2S and H_2O frozen in SO_2, *Icarus* **83**, 66–82, 1990.

Sartoretti, P., M. A. McGrath, and F. Paresce, Disk-resolved imaging of Io with the Hubble Space Telescope, *Icarus* **108**, 272–284, 1994.

Schaber, G. G., The geology of Io, in *Satellites of Jupiter*, D. Morrison (ed), University of Arizona Press, pp. 556–597, 1982.

Schenk, P., H. Hargitai, R. Wilson, A. McEwen, and P. Thomas, The mountains of Io: Global and geological perspectives from *Voyager* and *Galileo*, *J. Geophys. Res.* **106**, 33 201–33 222, 2001.

Schenk, P., R. Wilson, and R. Davies, Shield volcano topography and the rheology of lavas on Io, *Icarus* **in press**, 2003.

Schenk, P. M. and M. H. Bulmer, Origin of mountains on Io by thrust faulting and large-scale mass movements, *Science* **279**, 1514, 1998.

Schenk, P. M., A. McEwen, A. G. Davies, T. Davenport, K. Jones, and B. Fessler, Geology and topography of Ra Patera, Io, in the *Voyager* era: Prelude to eruption, *Geophys. Res. Lett.* **24**, 2467, 1997.

Schmitt, B. and S. Rodriguez, Identification of local deposits of Cl_nSO_2 (n = 1 or 2) on Io from NIMS/*Galileo* spectra, *J. Geophys. Res.* **in press**, 2003.

Schubert, G., D. J. Stevenson, and K. Ellsworth, Internal structures of the Galilean satellites, *Icarus* **47**, 46–59, 1981.

Segatz, M., T. Spohn, M. N. Ross, and G. Schubert, Tidal dissipation, surface heat flow, and figure of viscoelastic models of Io, *Icarus* **75**, 187–206, 1988.

Shirley, J. H., R. N. Clark, L. A. Soderblom, R. W. Carlson, L. W. Kamp, and *Galileo* NIMS Team, Io: Near-infrared absorptions not attributable to SO_2, *AAS/DPS* **33**, 0, 2001.

Showman, A. P. and R. Malhotra, The Galilean satellites, *Science* **286**, 77–84, 1999.

Simonelli, D. P. and J. Ververka, Bolometric albedos and diurnal temperatures of the brightest regions on Io, *Icarus* **74**, 240–261, 1988.

Simonelli, D. P., J. Veverka, and A. S. McEwen, Io: *Galileo* evidence for major variations in regolith properties, *Geophys. Res. Lett.* **24**, 2475, 1997.

Simonelli, D. P., C. Dodd, and J. Veverka, Regolith variations on Io: Implications for bolometric albedos, *J. Geophys. Res.* **106**, 33 241–33 252, 2001.

Sinton, W. M. and C. Kaminski, Infrared observations of eclipses of Io, its thermophysical parameters, and the thermal radiation of the Loki volcano and environs, *Icarus* **75**, 207–232, 1988.

Skinner, B. J., A sulfur lava flow on Mauna Loa, *Pacific Magazine* **24**, 44–145, 1970.

Smith, B. A., L. A. Soderblom, T. V. Johnson, A. P. Ingersoll, S. A. Collins, E. M. Shoemaker, G. E. Hunt, H. Masursky, M. H. Carr, M. E. Davies, A. F. Cook, J. M. Boyce, T. Owen, G. E. Danielson, C. Sagan, R. F. Beebe, J. Veverka, J. F. McCauley, R. G. Strom, D. Morrison, G. A. Briggs, and V. E. Suomi, The Jupiter system through the eyes of *Voyager 1*, *Science* **204**, 951–957, 1979.

Smythe, W. D., R. M. Nelson, and D. B. Nash, Spectral evidence for SO_2 frost or adsorbate on Io's surface, *Nature* **280**, 766, 1979.

Smythe, W. D., R. Lopes, S. Douté, S. W. Kieffer, R. Carlson, L. Kamp, and F. E. Leader, Evidence for a topographically controlled sulfur dioxide deposit at Chaac caldera, Io, in *EOS*, pp. A13+, 2001.

Smythe, W. D., R. Lopes-Gautier, and S. W. Kieffer, The effect of volatile content on plumes and flows on Io, *Icarus* **submitted**, 2002.

Soderblom, L., T. Johnson, D. Morrison, E. Danielson, B. Smith, J. Veverka, A. Cook, C. Sagan, P. N. Kupferman, D. Pieri, J. A. Mosher, C. Avis, J. Gradie, and T. Clancy, Spectrophotometry of Io: Preliminary *Voyager 1* results, *Geophys. Res. Lett.* **7**, 963–966, 1980.

Spencer, J. R. and N. M. Schneider, Io on the eve of the *Galileo* mission, *Ann. Rev. Earth Planet. Sci.* **24**, 125–190, 1996.

Spencer, J. R., A. S. McEwen, M. A. McGrath, P. Sartoretti, D. B. Nash, K. S. Noll, and D. Gilmore, Volcanic resurfacing of Io: Post-repair HST imaging, *Icarus* **127**, 221–237, 1997a.

Spencer, J. R., J. A. Stansberry, C. Dumas, D. Vakil, R. Pregler, M. Hicks, and K. Hege, History of high-temperature Io volcanism: February 1995 to May 1997, *Geophys. Res. Lett.* **24**, 2451, 1997b.

Spencer, J. R., K. L. Jessup, M. A. McGrath, G. E. Ballester, and R. Yelle, Discovery of gaseous S_2 in Io's Pele plume, *Science* **288**, 1208–1210, 2000a.

Spencer, J. R., J. A. Rathbun, L. D. Travis, L. K. Tamppari, L. Barnard, T. Z. Martin, and A. S. McEwen, Io's thermal emission from the *Galileo* Photopolarimeter-Radiometer, *Science* **288**, 1198–1201, 2000b.

Spencer, J. R., F. Bagenal, A. G. Davies, I. de Pater, F. Herbert, R. R. Howell, L. P. Keszthelyi, R. M. C. Lopes, M. A. McGrath, M. P. Milazzo, J. Moses, J. Perry, J. Radebaugh, J. A. Rathbun, N. M. Schneider, G. Schubert, W. Smythe, R. J. Terrile, E. P. Turtle, and D. A. Williams, The future of Io exploration, in *The Future of Solar System Exploration (2003–2013): First Decadal Study Contributions*, pp. 201–216, 2002a.

Spencer, J. R., J. A. Rathbun, A. S. McEwen, J. C. Pearl, A. Bastos, J. Andrade, M. Correia, and S. Barros, A new determination of Io's heat flow using diurnal heat balance constraints, in *Lunar and Planetary Science Conference Abstracts*, vol. 33, p. 1831, 2002b.

Spohn, T., Tides of Io, in *Tidal Phenomena*, p. 345, 1997.

Stansberry, J. A., J. R. Spencer, R. R. Howell, C. Dumas, and D. Vakil, Violent silicate volcanism on Io in 1996, *Geophys. Res. Lett.* **24**, 2455, 1997.

Stevenson, D. J. and S. C. McNamara, Background heatflow on hotspot planets: Io and Venus, *Geophys. Res. Lett.* **15**, 1455–1458, 1988.

Strom, R. G. and N. M. Schneider, Volcanic eruption plumes on Io, in *Satellites of Jupiter*, D. Morrison (ed), University of Arizona Press, pp. 598–633, 1982.

Tackley, P. J., G. Schubert, G. A. Glatzmaier, P. Schenk, J. T. Ratcliff, and J.-P. Matas, Three-dimensional simulations of mantle convection in Io, *Icarus* **149**, 79–93, 2001.

Turtle, E. P., W. L. Jaeger, L. P. Keszthelyi, A. S. McEwen, M. Milazzo, J. Moore, C. B. Phillips, J. Radebaugh, D. Simonelli, F. Chuang, and Peter Schuster *Galileo* SSI Team, Mountains on Io: High-resolution *Galileo* observations, initial interpretations, and formation models, *J. Geophys. Res.* **106**, 33 175–33 200, 2001.

Veeder, G. J., D. L. Matson, T. V. Johnson, D. L. Blaney, and J. D. Goguen, Io's heat flow from infrared radiometry: 1983-1993, *J. Geophys. Res.* **99**, 17 095–17 162, 1994.

Wienbruch, U. and T. Spohn, A self sustained magnetic field on Io?, *Planet. Space Sci.* **43**, 1045–1057, 1995.

Williams, D. A., A. H. Wilson, and R. Greeley, A komatiite analog to potential ultramafic materials on Io, *J. Geophys. Res.* **105**, 1671–1684, 2000.

Williams, D. A., A. G. Davies, L. P. Keszthelyi, and R. Greeley, The summer 1997 eruption at Pillan Patera on Io: Implications for ultrabasic lava flow emplacement, *J. Geophys. Res.* **106**, 33 105–33 120, 2001a.

Williams, D. A., R. Greeley, R. M. C. Lopes, and A. G. Davies, Evaluation of sulfur flow emplacement on Io from *Galileo* data and numerical modeling, *J. Geophys. Res.* **106**, 33 161–33 174, 2001b.

Witteborn, F. E., J. D. Bregman, and J. B. Pollack, Io: An intense brightening near 5 micrometers, *Science* **203**, 643–646, 1979.

Wong, M. C. and R. E. Johnson, A three-dimensional azimuthally symmetric model atmosphere for Io: 2. Plasma effect on the surface, *J. Geophys. Res.* **101**, 23 255–23 260, 1996.

Young, A. T., No sulfur flows on Io, *Icarus* **58**, 197–226, 1984.

Zahnle, K., L. Dones, and H. F. Levison, Cratering rates on the Galilean satellites, *Icarus* **136**, 202–222, 1998.

Zhang, J., D. B. Goldstein, P. L. Varghese, N. E. Gimelshein, D. A. Levin, and S. F. Gimelshein, Modeling low density sulfur dioxide volcanoes on Jupiter's moon Io, in *Lunar and Planetary Science Conference Abstracts*, vol. 33, p. 1137, 2002.

Zolotov, M. Y. and B. Fegley, Oxidation state of volcanic gases and the interior of Io, *Icarus* **141**, 40–52, 1999.

Zolotov, M. Y. and B. J. Fegley, Eruption conditions of Pele volcano on Io inferred from chemistry of its volcanic plume, *Geophys. Res. Lett.* **27**, 2789, 2000.